AFML-TR-68-90
Part II

VISCOELASTIC BEHAVIOR OF A NONLINEAR, FIBER-REINFORCED PLASTIC

Y. C. Lou

R. A. Schapery

Note for Part I in book acc #71927

PURDUE UNIVERSITY

TECHNICAL REPORT AFML-TR-68-90, PART II

APRIL 1969

AIR FORCE MATERIALS LABORATORY
AIR FORCE SYSTEMS COMMAND
WRIGHT-PATTERSON AIR FORCE BASE, OHIO 45433

DISCLAIMER NOTICE

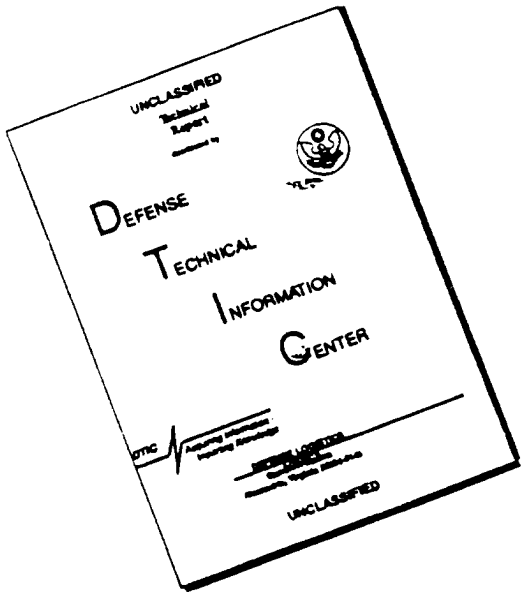

THIS DOCUMENT IS BEST QUALITY AVAILABLE. THE COPY FURNISHED TO DTIC CONTAINED A SIGNIFICANT NUMBER OF PAGES WHICH DO NOT REPRODUCE LEGIBLY.

NOTICES

When Government drawings, specifications, or other data are used for any purpose other than in connection with a definitely related Government procurement operation, the United States Government thereby incurs no responsibility nor any obligation whatsoever; and the fact that the Government may have formulated, furnished, or in any way supplied the said drawings, specifications, or other data, is not to be regarded by implication or otherwise as in any manner licensing the holder or any other person or corporation, or conveying any rights or permission to manufacture, use, or sell any patented invention that may in any way be related thereto.

This report has been approved for public release and sale; its distribution is unlimited.

Copies of this report should not be returned to the Aeronautical Systems Division unless return is required by security considerations, contractual obligations, or notice on a specific document.

FOREWORD

This report was prepared by Purdue Research Foundation, Lafayette, Indiana, under USAF Contract F33615-67-C-1412. The contract was initiated under Project No. 7342, "Fundamental Research on Macromolecular Materials and Lubrication Phenomena," Task No. 734202, "Studies on the Structure-Properties Relationships of Polymeric Materials." The work was administrated by the Elastomers and Coatings Branch, Nonmetallic Materials Division, Air Force Materials Laboratory, with Mr. J. C. Halpin, MANE, as project scientist. This report, prepared under Purdue Research Foundation, Project No. 4958, covers the period from 1 January 1968 to 31 December 1968, and was released by the authors February 1969 for publication.

This report has been reviewed and is approved.

W. P. JOHNSON, Chief
Elastomers and Coatings Branch
Nonmetallic Materials Division
Air Force Materials Laboratory

ABSTRACT

The nonlinear mechanical properties of a unidirectional, glass fiber-epoxy composite at 164°F are characterized by using creep and recovery tests together with a constitutive equation based on a thermodynamic theory. Our experimental effort covers studies on specimens with fiber orientations at $\theta = 0^\circ$, 30°, 45°, 60° and 90° with respect to the uniaxial loading direction. The results for $\theta = 0^\circ$ specimen show that the composite is linearly elastic for the load range studied, but nonlinear viscoelastic behavior is observed for the other orientations. Guided by the nonlinear constitutive equation, the creep and recovery data are plotted on double-logarithmic paper, and the material properties are found by shifting the data to form a "master curve" for each fiber orientation. Prediction of master curves of $\theta = 45^\circ$ and 60° from master curves of $\theta = 0^\circ$, 90° and 30° is made. Four principal creep compliances are estimated by using the master curves and tensor transformation relations. Finally, we use the nonlinear equation to predict strain response due to multiple-step loading and unloading.

The Appendix contains two abstracts of papers which were completed and published during the period covered by this report.

TABLE OF CONTENTS

ILLUSTRATIONS

Section I

INTRODUCTION

Nonlinear viscoelastic behavior of a unidirectional, glass fiber-epoxy composite under controlled loading and at approximately 164°F and 21% relative humidity is studied. The nonlinear constitutive equation which is used here has been derived from thermodynamic theory [1]* and is similar to the Boltzmann superposition integral of linear viscoelastic theory.

Special cases of this nonlinear theory have been applied with limited success by other investigators to characterize monolithic polymeric materials. For example, Leaderman proposed and applied to fibers a so-called modified superposition principle (MSP) [2]. Recently, Findley and Lai [3] used a MSP to predict strain response of unplasticized PVC to discontinuously applied tensile and shearing stresses. In a more recent paper [4] the various nonlinear theories are reviewed, and the type of theory used here is applied to experimental data on different materials under controlled loading and controlled straining.

In Section II, linear and nonlinear constitutive equations for uniaxial loading are given. An equation for the average octahedral shear stress in the epoxy matrix is also derived for later reference.

The specimen and experimental equipment are described in Section III. Creep and recovery data for various loads and fiber angles are then given. It is shown, using the nonlinear theory, that a graphical shifting procedure

---

* Numbers in square brackets indicate references at end of report.

can be used to reduce both the nonlinear creep and the recovery data plotted on double-logarithmic paper. This procedure provides master curves which, for the creep period, are simply the time-dependent linear viscoelastic creep compliances. Stress-dependent nonlinear properties are determined by the amount of vertical and horizontal shifting needed to form the master curves; we find these properties depend primarily on the average octahedral shear stress in the epoxy. How well data form master creep and recovery curves provides an indication of the validity of the theory. The results reported herein do indeed verify the theory in that good master curves are obtained. Prediction of linear viscoelastic compliances at $\theta = 45^{\circ}$ and 60° from the curves of $\theta = 0^{\circ}$, 90° and 30°, are then made by using tensor transformation relations.

In Section IV the principal creep compliances are estimated. Finally, strain response due to multiple-step loading is predicted in Section V using the nonlinear constitutive equation and the material properties found from creep and recovery data. Good agreement between theory and experiment is achieved during most of the time range covered.

Section II

CONSTITUTIVE THEORY

1. LINEAR CONSTITUTIVE EQUATION

The Boltzmann superposition integral can be used to represent the stress-strain relation for linear viscoelastic materials. Strain response, ε, to an arbitrary stress input, σ, is

$$\varepsilon = \int_0^t A(t-\tau)\frac{d\sigma}{d\tau}\, d\tau \tag{1a}$$

or, equivalently,

$$\varepsilon = A(0)\sigma + \int_0^t \Delta A(t-\tau)\frac{d\sigma}{d\tau}\, d\tau \tag{1b}$$

where $A(t)$ is the creep compliance; it is defined as the strain output due to a unit step stress input, $\sigma = H(\tau)$, and

$$H(\tau) = \begin{cases} 0 & \tau < 0 \\ 1 & \tau > 0 \end{cases} \tag{2}$$

The range of integration in (1) includes the stress discontinuity that occurs at $t = 0$ in a creep test. $A(0)$ is the initial value of creep compliance and $\Delta A(t)$ is the transient component of creep compliance, $\Delta A(t) = A(t) - A(0)$.

The linear viscoelastic compliance $A(t)$ is a function of the angle between fiber and loading axis, θ. Later, we shall use the notation A_θ

to bring out this angular dependence.

When a constant stress σ_o is applied at $t = 0$ and removed at $t = t_1$, viz.,

$$\sigma = \sigma_o[H(\tau) - H(\tau-t_1)] \tag{3}$$

we have a so-called "creep and recovery test."

Substituting (3) into (1b), the stress-strain relation for the creep period, $0 < t < t_1$, is

$$\varepsilon = A(0)\sigma_o + \Delta A(t)\sigma_o = A(t)\sigma_o \tag{4}$$

while during recovery, $t > t_1$, it is

$$\varepsilon_r = \varepsilon(t) - \varepsilon(t-t_1) \tag{5a}$$

or, equivalently,

$$\varepsilon_r = [\Delta A(t) - \Delta A(t-t_1)]\sigma_o \tag{5b}$$

In (5), ε_r is the strain measured after the removal of the stress, and $\varepsilon(t)$ is the creep strain for $t > t_1$ which would exist if the stress had not been removed at $t = t_1$. The familiar relation between creep and recovery predicted by equation (5) for a linear viscoelastic material is shown in Figure 1.

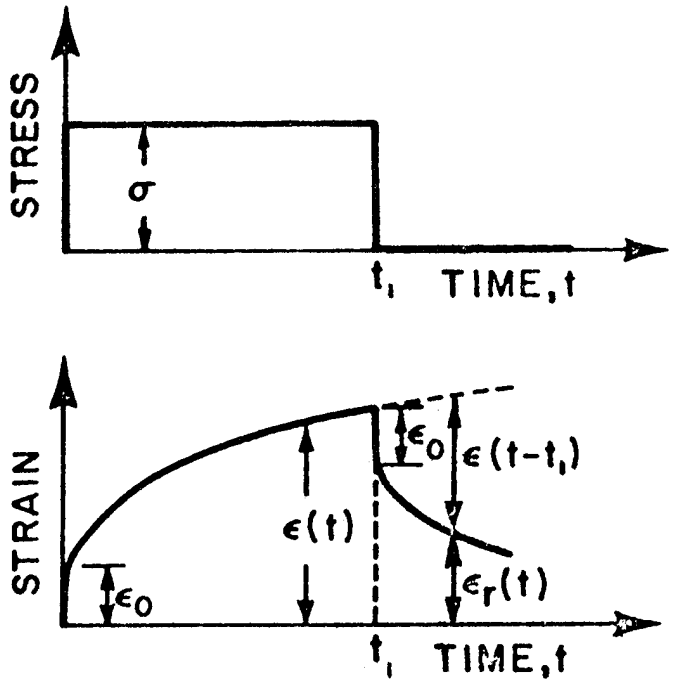

Figure 1.

Relation Between Creep and Recovery
for a Linear Viscoelastic Material

2. NONLINEAR CONSTITUTIVE EQUATION

The nonlinear constitutive equation derived in [1] is

$$\varepsilon = g_o A(0)\sigma + g_1 \int_o^t \Delta A(\psi-\psi') \frac{dg_2\sigma}{d\tau}\, d\tau \qquad (6)$$

where $A(\psi) = A(0) + \Delta A(\psi)$ is still the linear creep compliance and ψ is the so-called "reduced-time" defined by

$$\psi = \int_o^t d\tau'/a_\sigma[\sigma(\tau')] \qquad (7a)$$

$$\psi' \equiv \psi(\tau) = \int_o^\tau d\tau'/a_\sigma[\sigma(\tau')] \qquad (7b)$$

and the material properties g_o, g_1, g_2 and a_σ are functions of stress input. When the material is loaded within the linear range, $g_o = g_1 = g_2 = a_\sigma = 1$, and equation (6) becomes the Boltzmann superposition integral (1).

The modified superposition principal proposed by Leaderman [2] can be derived from equation (6) by setting $g_o = g_1 = a_\sigma = 1$; it is

$$\varepsilon = A(0)\sigma + \int_o^t \Delta A(t-\tau) \frac{dg_2\sigma}{d\tau}\, d\tau \qquad (8)$$

The thermodynamic significance of changes in g_o, g_1 and g_2 is that they reflect third and higher order stress dependence of the Gibb's free energy, while a_σ arises from similar strong stress effects in both entropy production and free energy.

When a step stress input $\sigma = \sigma_o[H(\tau) - H(\tau-t_1)]$ is applied, equation (6) yields,

$$\varepsilon = g_o A(0)\sigma_o + g_1 g_2 A(\frac{t}{a_\sigma})\sigma_o , \quad 0 < t < t_1 \tag{9a}$$

$$\varepsilon_r = g_2[\Delta A(\psi) - \Delta A(\psi-\psi_1)]\sigma_o , \quad t_1 < t \tag{9b}$$

where in (9b)

$$\psi_1 = t_1/a_\sigma , \quad \psi = t_1/a_\sigma + t-t_1$$

Notice that $\varepsilon \equiv \varepsilon_1 = g_o A(0)\sigma_o + g_1 g_2 \Delta A(\psi_1)\sigma_o$ immediately before the load is removed, and $\varepsilon \equiv \varepsilon_1' = g_2 \Delta A(\psi_1)\sigma_o$ immediately after the load is removed. Therefore the jump in strain at $t = t_1$ is

$$\Delta\varepsilon_1 = \varepsilon_1-\varepsilon_1' = g_o A(0)\sigma_o + (g_1-1)g_2 \Delta A(\psi_1)\sigma_o \tag{10}$$

It is important to notice that the strain jump at $t = 0$, $\varepsilon(0) = g_o A(0)\sigma_o$ is not necessarily equal to the jump at $t = t_1$, $\Delta\varepsilon_1$. It is clear from equation (10) that these two jumps are equal only when $g_1 = 1$; the linear viscoelastic material has the same jump in strain during both loading and unloading since $g_1 = 1$ in the linear range.

3. OCTAHEDRAL SHEAR STRESS

The linear viscoelastic creep compliances are the only time-dependent material properties in the theory used here. Other material properties are stress-dependent functions, and from our experimental results we find that they can be expressed approximately as a function of a single invariant: the average octahedral shear stress in the epoxy matrix. That the octahedral

shear stress is the main function needed to characterize nonlinear behavior is suggested by multiaxial creep data on plastics and metals [4]. For later reference purposes, we shall develop this invariant here in terms of applied stress and fiber angle.

Octahedral shear stress is defined as the shear stress which acts on a plane whose normal makes equal acute angles with the positive principal stress directions. It is [5]

$$\tau_{oct} = \frac{1}{3}[(\sigma_1-\sigma_2)^2 + (\sigma_2-\sigma_3)^2 + (\sigma_3-\sigma_1)^2]^{1/2} \qquad (11)$$

where σ_1, σ_2 and σ_3 are the principal stresses.

Consider now a composite specimen with fiber orientation θ, under a uniaxial stress σ, which is shown in Figure 2. The average (applied) stresses normal to the fiber, σ_f, and along the fiber, σ_f', and also the average shear stress along the fiber, τ_f, are found using the usual tensor transformation relations:

$$\sigma_f = \sigma \sin^2\theta \qquad (12a)$$

$$\sigma_f' = \sigma \cos^2\theta \qquad (12b)$$

$$\tau_f = \frac{\sigma}{2} \sin 2\theta \qquad (12c)$$

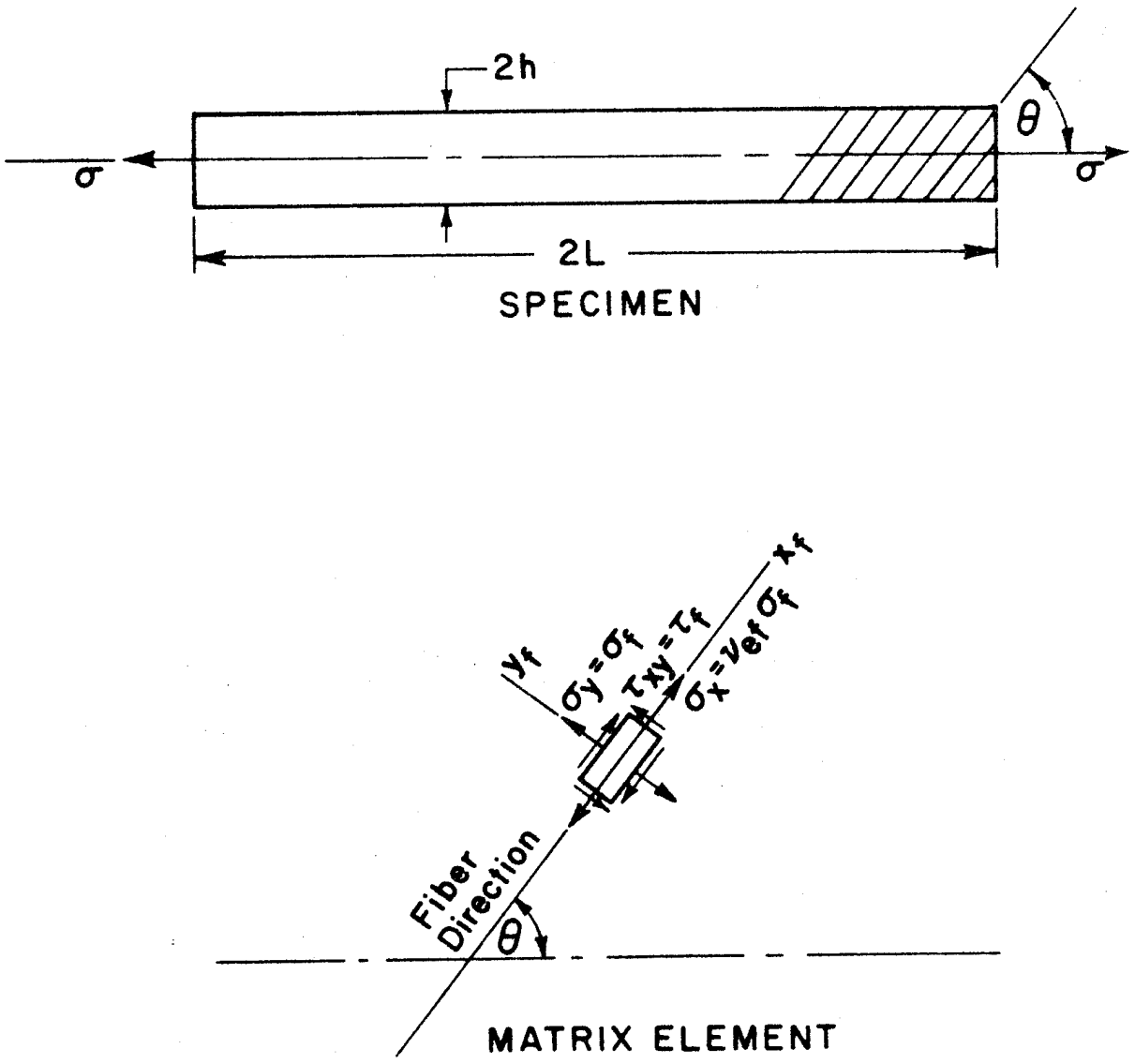

Figure 2.

Diagram for Derivation of Octahedral Shear Stress

The average stress state of the matrix element is plane stress; viz. $\sigma_z = \tau_{xz} = \tau_{yz} = 0$. Furthermore, if we assume the fibers are so relatively stiff that $\varepsilon_x \approx 0$, the average stress on the matrix element due to σ becomes,

$$\sigma_y = \sigma_f \tag{13a}$$

$$\sigma_x = \nu_e \sigma_y = \nu_e \sigma_f \tag{13b}$$

$$\tau_{xy} = \tau_f \tag{13c}$$

where ν_e is defined as the ratio σ_x/σ_f; it is equal to the matrix Poisson's ratio in the linear range only. However, it turns out the result is quite insensitive to ν_e, and therefore the linear elastic value will be used in reducing our data.

Octahedral shear stress is found from the stresses (13) and equation (11) to be

$$\tau_{oct} = \frac{\sqrt{2}}{\sqrt{3\gamma}} [\sigma_f^2 + \gamma \tau_f^2]^{1/2} \tag{14a}$$

where

$$\gamma = \frac{3}{1 - \nu_e + \nu_e^2} \tag{14b}$$

We find γ has a maximum value of 4 when $\nu_e = 0.5$.

Because the fibers are not infinitely rigid, ε_x is not actually zero. Instead, it equals $A_{11}\sigma_f' + A_{12}\sigma_f$, and corrected stresses on the matrix element are

$$\sigma_y = \sigma_f \tag{15a}$$

$$\sigma_x = (E_e A_{11}\cot^2\theta + E_e A_{12} + \nu_e)\sigma_f = \nu_{ef}\sigma_f \tag{15b}$$

$$\tau_{xy} = \tau_f \tag{15c}$$

where $\nu_{ef} = E_e A_{11}\cot^2\theta + E_e A_{12} + \nu_e$

E_e is the modulus of the epoxy, and A_{11} and A_{12} are principal composite compliance components along the fiber and transverse to the fiber, respectively.

The same octahedral shear stress form (14) is obtained by using the stress distribution (15) and equation (11), except the effective Poisson's ratio ν_{ef} is used instead of the epoxy Poisson's ratio ν_e.

If we use typical epoxy properties

$$\nu_e = 0.35 \qquad E_e = 0.5 \times 10^6 \text{ psi}$$

and the composite properties which we will find later from our experimental data ($A_{11} = .184 \times 10^{-6}$ psi^{-1} and $A_{12} = -.057 \times 10^{-6}$ psi^{-1}) it is found that $\gamma = 3.88$ when ν_e is used. For the specimens studied, the biggest error in γ due to the use of ν_e instead of ν_{ef} is 2.1% which occurs when $\theta = 45^\circ$. This small amount of error in γ affects the octahedral shear stress only slightly, so that the equation (14) will be used. We should add that a quantity σ_e,

$$\sigma_e \equiv \tau_{oct}\frac{\sqrt{3\gamma}}{\sqrt{2}} = [\sigma_f^2 + \gamma\tau_f^2]^{1/2} \tag{16}$$

will actually be used in reducing data, for convenience. This invariant is sometimes called the effective stress. It is observed that $\sigma_e = \sigma_f$ when the matrix itself is under a uniaxial stress equal to σ_f.

Section III

EXPERIMENTAL WORK AND DATA REDUCTION

1. SPECIMEN AND EQUIPMENT

The contracting agency supplied the unidirectional, glass fiber-epoxy composite material. It was fabricated by contacting eight plies for five minutes and then applying a pressure of 25 psi for 35 minutes. A temperature of 330°F was maintained throughout the pressure cycle.

The composite has a density of 1.67 g/c.c., 62.4 weight percent fiber, and 47.6 volume percent fiber.

Five sets of specimens, with θ equal 0, 30, 45, 60, and 90 degrees, were cut to the nominal dimensions of 1/2" x 1/10" x 6" from the same large plate. Three specimens were cut at each angle. One of them served as a dummy to compensate the thermal expansion of the strain gage used, and the other two specimens were both tested in the test program of one hour creep and two hours recovery. Some difference was found between the specimens, mainly in the initial (elastic) response; since the largest difference in elastic response was found to be only 3.4%, which occured for $\theta = 30^{\circ}$, data from one specimen at each angle was chosen for data reduction purposes.

The equipment used is shown in Figure 3. A Develco Environmental chamber is shown inside the ARA* loading frame toward the right center. Two Budd Model TC-22 Digital Strain indicators are used to record strains, and they are shown in the left center. A Bristol temperature and humidity controller is on the right side while on the left side is the control panel

* Allied Research Associates, Inc.

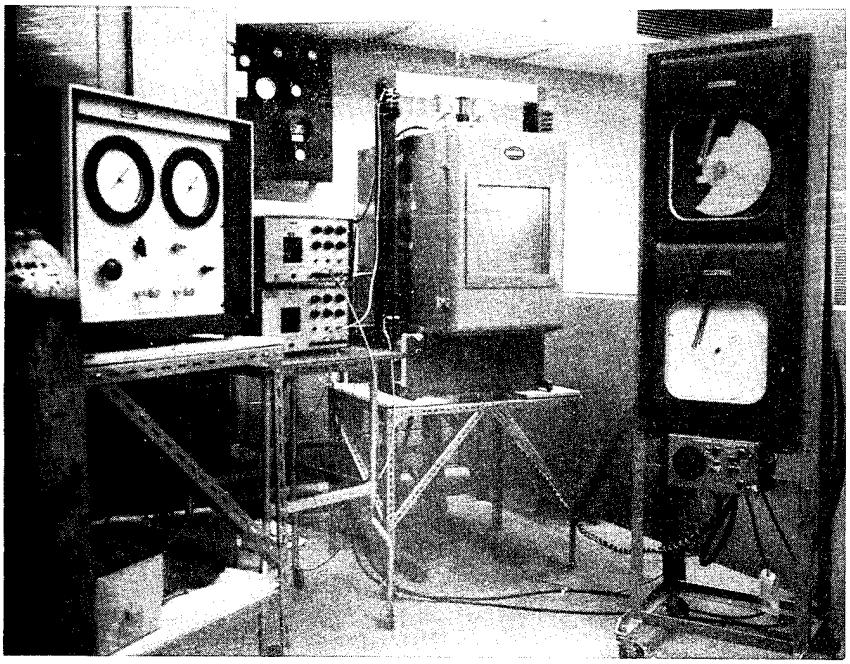

Figure 3

Testing Equipment

of the ARA Precision Pneumatic Testing Machine. A nitrogen tank is shown at the left corner to supply pneumatic pressure for the ARA Testing Machine, which has a loading capacity of 1800 pounds.

In Figure 4, a close-up view of the specimen inside the chamber is shown; the specimen is arranged vertically between grips. (A plate in the background makes the specimen appear to be bent).

Two BLH* strain gages (FAER-25R-35-S13) are mounted on the specimen. They are placed along the longitudinal direction of the specimen, one on each side and connected in series to average out the bending. For 0 and 90 degree specimens, an additional gage is placed along the transverse direction to measure the transverse strain directly. Each gage has high resistance of 350 Ohms. Eastman 910 is used as the bonding agent, which has a maximum allowable temperature of 250°F.

It was found that during the early testing period of each specimen the strain due to a given load decreased with successive tests. After five to ten cycles repeating the loading and unloading process, the specimen became stable in creep compliance. For example, a stress of 2690 psi was applied to condition our 60 degree specimen. We found that total strain output under a one hour loading creep test is reduced by 3% after several cycles.

This reduction in compliance may be due to the arrest of cracks which form in the matrix under initial load application. That cracks do indeed develop in the rigid matrix has been discussed by Halpin [6].

---

* Baldwin-Lima-Hamilton Corporation

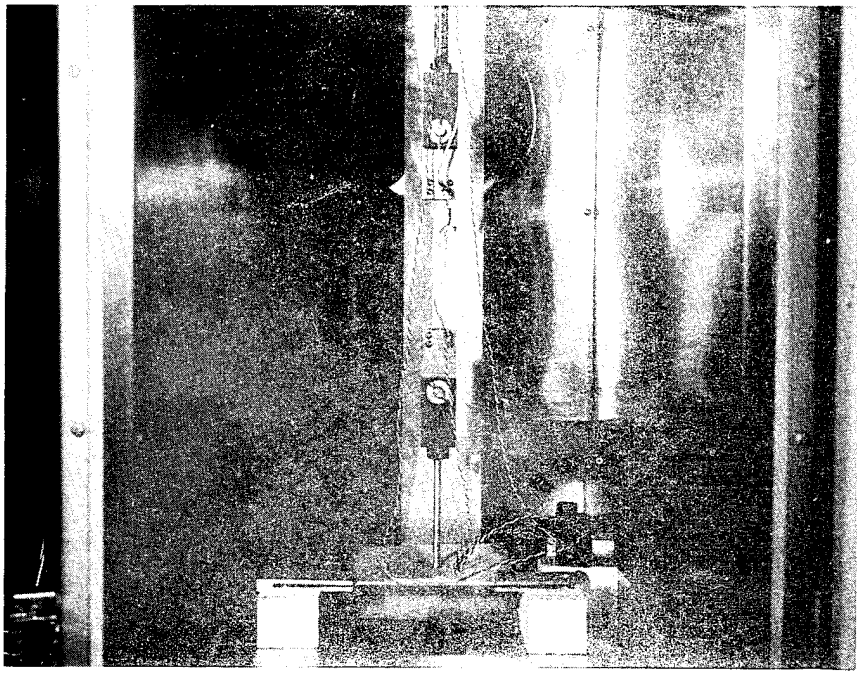

Figure 4

Specimen Inside the Environmental Chamber

2. EQUATIONS FOR LINEAR VISCOELASTIC COMPLIANCES

For a linear viscoelastic material under constant stresses, and in a state of plane stress in the x-y plane, the strain-stress relations for any fiber orientation, θ, relative to the x axis are

$$\varepsilon_x = A'_{11}\sigma_x + A'_{12}\sigma_y + A'_{16}\tau_{xy} \tag{17a}$$

$$\varepsilon_y = A'_{21}\sigma_x + A'_{22}\sigma_y + A'_{26}\tau_{xy} \tag{17b}$$

$$\gamma_{xy} = A'_{61}\sigma_x + A'_{62}\sigma_y + A'_{66}\tau_{xy} \tag{17c}$$

(In all of our discussions the fibers are assumed to be in the x-y plane.)

The elements A'_{ij} are the creep compliances at this particular value of θ. They form a fourth order tensor, so that the relation between the creep compliances of different fiber orientations θ follows the usual tensor transformation law [7].

For a state of plane stress, only four principal creep compliances A_{11}, A_{12}, A_{22} and A_{66} are needed to characterize the composite; the principal directions are parallel to and normal to the fibers. When the x-y axes are these principle axes, the stress-strain relations become

$$\varepsilon_x = A_{11}\sigma_x + A_{12}\sigma_y \tag{18a}$$

$$\varepsilon_y = A_{21}\sigma_x + A_{22}\sigma_y \tag{18b}$$

$$\gamma_{xy} = A_{66}\tau_{xy} \tag{18c}$$

Pagano and Halpin [8] derived an axial compliance of a tensile specimen which is clamped at both ends:

$$A_\theta \equiv \frac{\varepsilon}{\sigma} \equiv A'_{11}\left[\frac{6A'_{11}A'_{66} + A'^{2}_{11}\frac{L^2}{h^2} - 6A'_{16}}{6A'_{11}A'_{66} + A'^{2}_{11}\frac{L^2}{h^2}}\right] \qquad (19)$$

where A'_{11}, A'_{16} and A'_{66} are the components of the creep compliance tensor at this angle θ, while 2L and 2h are the length and width of the specimen, respectively; the complexity of this equation results from specimen bending when $\theta \neq 0^\circ$ and $\theta \neq 90^\circ$. If the specimen is sufficiently long compared to its width ($\frac{h}{L} << 1$), equation (19) becomes

$$A_\theta \equiv \frac{\varepsilon}{\sigma} \simeq A'_{11} \qquad (20)$$

This approximation will be used in all of our data reduction of linear and nonlinear data, and will be verified numerically later in the paper.

3. 0 DEGREE SPECIMEN

Negligible creep has been found when loaded along the fibers ($\theta = 0^\circ$) at 164°F and 21% relative humidity, with a stress range from 1376 psi to 6881 psi. The axial strain output ε_o due to uniaxial loading $\sigma \equiv \sigma_x$ is linearly elastic, which is shown in Figure 5. The directly measured axial compliance, A_o, is equal to the principal creep compliance A_{11},

$$A_{11} = A_o = \frac{\varepsilon_o}{\sigma_x} = .184 \times 10^{-6} \ (\text{psi}^{-1})$$

The lateral strain ε_y due to the axial stress σ_x is also found to be linear and independent of time; from equation (18b) the principal creep compliance A_{21} is

$$A_{21} = \frac{\varepsilon_y}{\sigma_x} = - .060 \times 10^{-6} \ (\text{psi}^{-1})$$

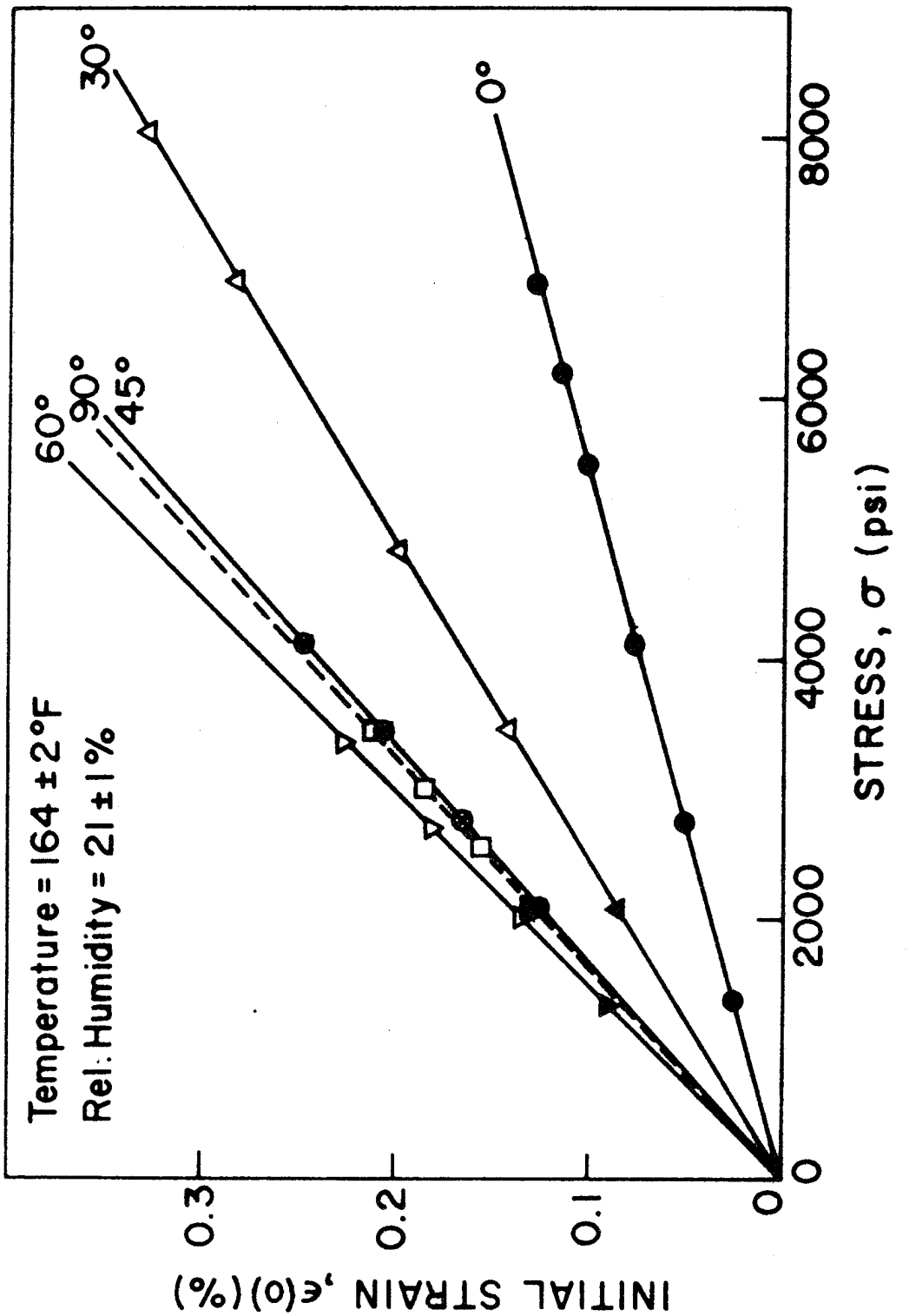

Figure 5. Initial Strain

The Poisson's ratio of the composite transverse to the fiber is

$$\nu_{21} = -\frac{\varepsilon_y}{\varepsilon_o} = .327$$

4. OFF-ANGLE SPECIMENS

The analytical expression for the nonlinear creep compliance at any angle is obtained from equation (9a),

$$A_{\theta n} \equiv \frac{\varepsilon}{\sigma} = g_o A_\theta(0) + g_1 g_2 \Delta A_\theta(\psi) \tag{21}$$

where, for constant stress, $\psi = t/a_\sigma$

In another paper [4] a method for evaluating all property functions in (21) from creep and recovery data is given. Depending on whether or not $\Delta A_\theta(\psi)$ is a power law, somewhat different approaches are needed. Notice that when it is a power law, viz.

$$\Delta A_\theta(\psi) = c\psi^n \tag{22}$$

where c and n are constants, equation (21) yields

$$A_{\theta n} = g_o A_\theta(0) + c\,\frac{g_1 g_2}{a_\sigma^n}\, t^n \tag{23}$$

This shows that creep data will provide information for evaluating the combination $g_1 g_2/a_\sigma^n$, but not $g_1 g_2$ and a_σ separately. It turns out that the power law can indeed be used to fit our data. This power law representation has been reported for many plastics and metals [9].

a. Initial Compliance

In principle, creep data can be used to evaluate g_o and A(0) in equation (23); recall that $g_o = 1$ under sufficiently small stresses, and g_o therefore represents nonlinearity that may exist in the initial compliance.

However, we were unable to measure strain at a short enough time to obtain the initial compliance directly from the data in the nonlinear creep range of behavior. As a result, the following method was used to estimate the initial compliance.

For each fiber angle studied, we found our first strain reading (at approximately t = 3 seconds) is linear in stress when the stress is sufficiently small; this is approximately the same range for which recovery equation (5) is found to hold. The slope of this 3-second curve is assumed to be the initial creep compliance A(0). Motivated by the nonlinear creep behavior reported in [10] for a fiber-reinforced phenolic resin, in that $g_o = 1$ for all applied stresses, we assume this is also the case here. Graphs of the initial strain, $\varepsilon(0) = A(0)\sigma$ are shown in Figure 5. (The solid points are some measured values, while the open points are estimated values using the constant initial compliance and each stress value applied in the test program). The initial creep compliances, as given by the slopes of these lines, are

$$A_{30}(0) = 0.410 \times 10^{-6} \ (\text{psi}^{-1})$$

$$A_{45}(0) = 0.600 \times 10^{-6} \ (\text{psi}^{-1})$$

$$A_{60}(0) = 0.668 \times 10^{-6} \ (\text{psi}^{-1})$$

$$A_{90}(0) = 0.614 \times 10^{-6} \ (\text{psi}^{-1})$$

It is found that when the initial compliance determined above is subtracted from the total compliance, $A_{\theta n}$, the power law shown in (23) results. Even if our estimations of initial compliances are not valid for very short times, they should be acceptable as long as prediction of very short time response is not required for the engineering application of interest.

When $\theta = 90^{\circ}$, the initial creep compliance is equal to the principal compliance $A_{22}(0)$,

$$A_{22}(0) = A_{90}(0) = 0.614 \times 10^{-6} \ (\text{psi}^{-1})$$

Further, the lateral strain measurement ε_x due to a sufficiently small axial stress σ normal to the fibers ($\theta = 90^\circ$) gives the principal creep compliance A_{12} by using equation (18a). For the entire stress range studied, A_{12} is found to be essentially independent of time and stress, with the value

$$A_{12} = \frac{\varepsilon_x}{\sigma} = - 0.054 \times 10^{-6} \ (\text{psi}^{-1})$$

The initial Poisson's ratio of the composite for loading normal to fibers is found experimentally as

$$\nu_{12}(0) = - \frac{\varepsilon_x}{\varepsilon_o} = 0.088$$

Theory shows that $A_{12} = A_{21}$ [11]. However, we reported previously that $A_{21} = - .060 \times 10^{-6}$ (psi^{-1}); the approximately 10% difference between A_{12} and A_{21} can be attributed to experimental error, considering the very small strains involved. The average value will be used in characterizing the material,

$$A_{12} = A_{21} = - .057 \times 10^{-6} \ (\text{psi}^{-1})$$

The initial compliances are plotted against fiber angle in Figure 6; also shown is the one-hour compliance which will be discussed later.

In this Figure, compliances at $\theta = 0^\circ$, 90°, and 30° were used in fourth-order tensor transformation relations to predict compliances at $\theta = 45^\circ$ and 60°. Also shown are data for a second set of specimens, which brings out the specimen-to-specimen variation that exists, even though they are all cut out of the same plate. It is seen that noticeably better prediction of the 45° and 60° compliances would have been obtained if the larger compliance at 30° (solid point) had been used.

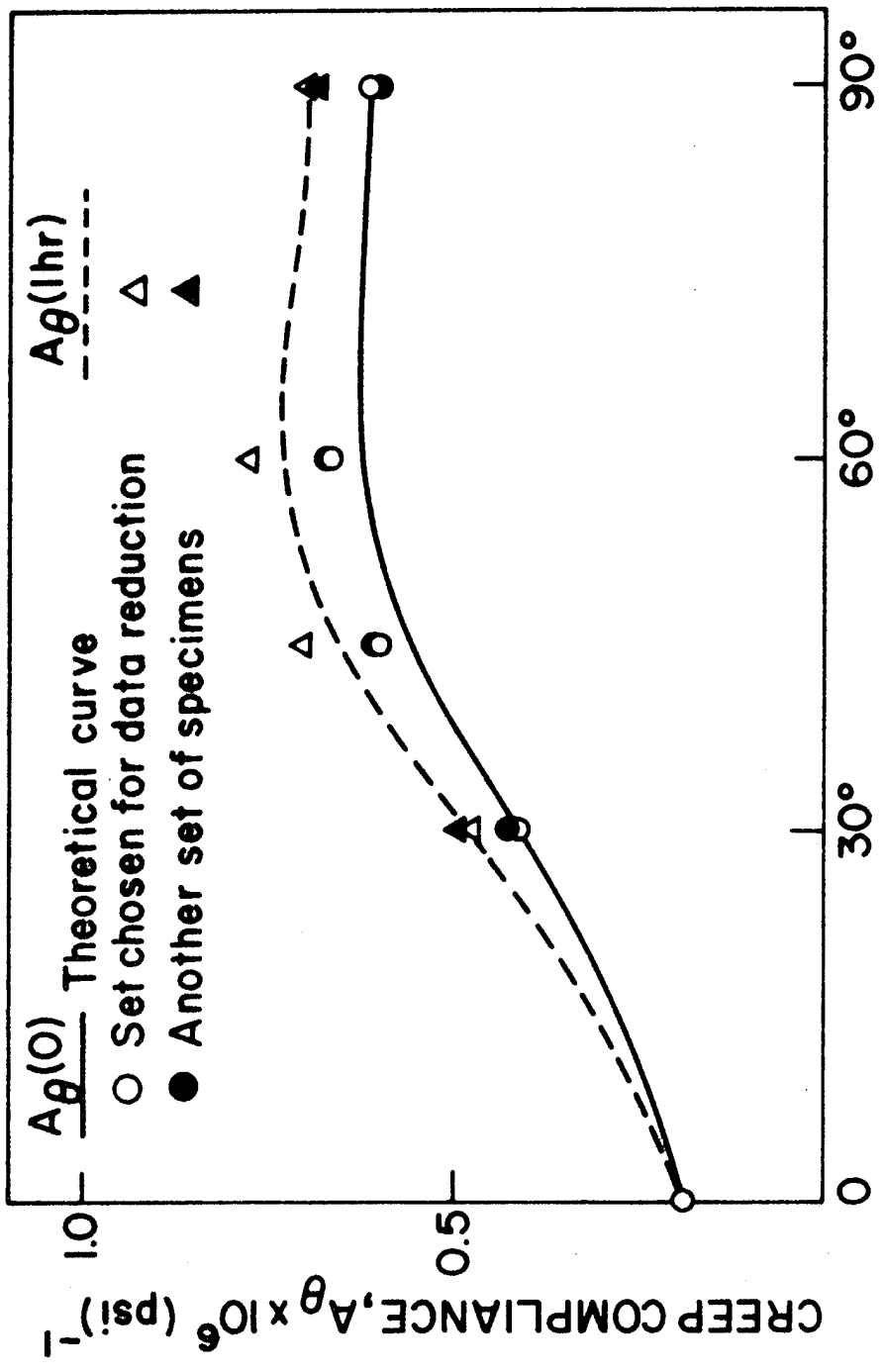

Figure 4. Angular Dependence of Creep Compliance

Some of the error in these predictions is probably due to inhomogeneity in the plate, as well as our method of estimating initial compliance.

b. Reduction of Creep Data

Most nonlinearity and creep occurred for the 30° specimen. We shall therefore use this fiber angle to discuss the details of data reduction.

Creep and recovery data on this specimen are shown in Figure 7. For comparison purposes we note that the ultimate tensile strength at 30° is approximately 10300 psi, and the material is nonlinear for $\sigma \tilde{>} 2000$ psi.

Equation (21) can be rewritten as

$$\Delta A_{\theta n} = A_{\theta n} - A_{\theta}(0) = g_1 g_2 \Delta A_{\theta}(t/a_{\sigma}) \tag{24}$$

and

$$\log \Delta A_{\theta n} = \log g_1 g_2 + \log \Delta A_{\theta}(t/a_{\sigma}) \tag{25}$$

where $\Delta A_{\theta n}$ is the transient component of the nonlinear creep compliance, ΔA_{θ} is the transient component of the linear creep compliance, and we have assumed $g_o = 1$.

We have plotted $\Delta A_{\theta n}$ against t on double-logarithmic paper in Figure 8. Nearly parallel straight lines are shown for different stress levels, with only a small slope difference existing at the lowest stress level (2069 psi). Linear viscoelastic relation (5) is found to be valid at this lowest stress, for which the material is considered to be approximately linear; we shall assume the material is linear for all stresses $\sigma \leq 2069$ psi. Recording error for the small strain output at low stress and the method used to estimate initial compliance might have caused the observed difference in slope.

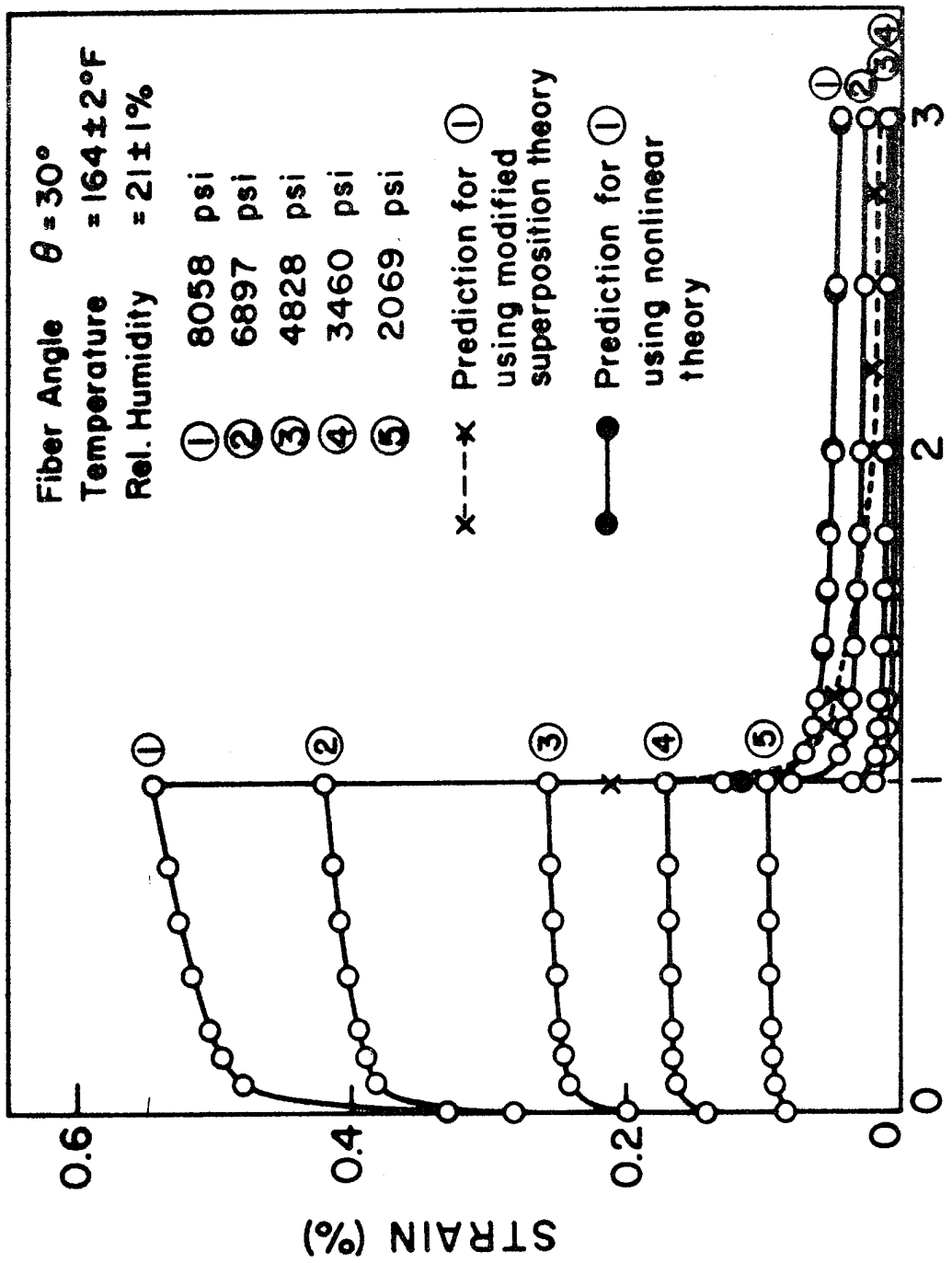

Figure 7. Creep-Recovery Curves ($\theta = 30^{\circ}$)

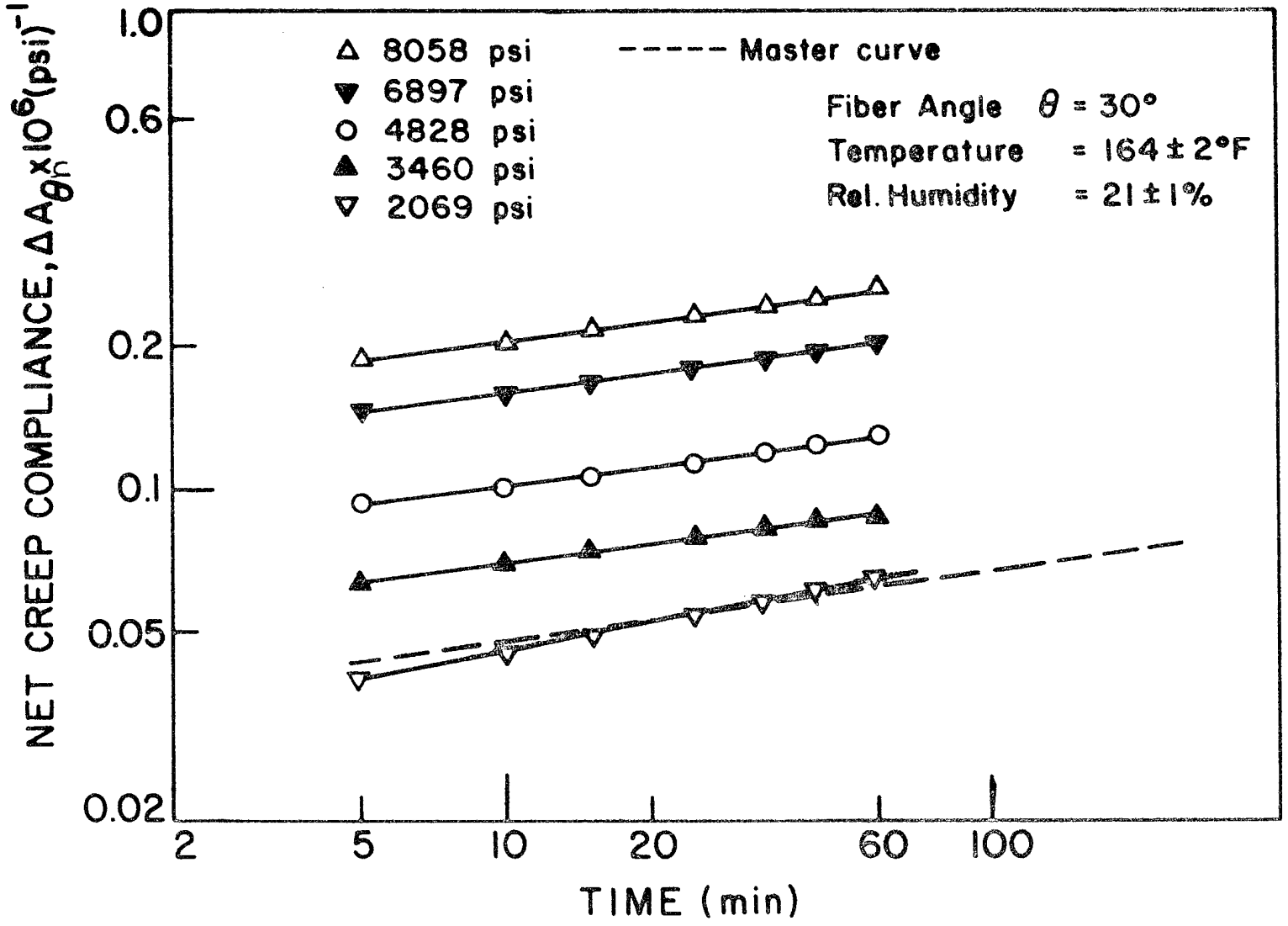

Figure 8. Net Creep Compliance for Different Stress Levels ($\theta = 30^0$)

It is clear that the data at different stress levels can be shifted along the two axes to a parallel straight line near the line at the lowest stress level, which is shown as the broken line in Figure 8. It is the so-called master curve, and is assumed to be the transient component of the linear viscoelastic creep compliance.

The amount of horizontal (t) shift and vertical (ΔA_{θ_n}) shift equals log a_σ and log $g_1 g_2$ respectively. Since the lines at different stress levels are parallel, straight lines, it is obvious that we cannot obtain unique values for a_σ and $g_1 g_2$ from the shift of the creep data; had curvature been found, the vertical and horizontal shifts would have been determined uniquely.

Additional information will be provided by recovery data in order to evaluate unique values of a_σ and $g_1 g_2$, and also g_1 and g_2 separately; this will be discussed in the next subsection.

Smaller nonlinearity is shown in Figure 9 for $\theta = 90^\circ$. Parallel, straight lines are also found for the creep compliance data at different stress levels for $\theta = 90^\circ$, as well as $\theta = 45^\circ$ and 60°.

c. Reduction of Recovery Data

The nearly parallel, straight lines on double-logarithmic paper shown in Figures 8 and 9 indicate that the power-law form can represent the linear creep compliance; namely,

$$A_\theta = A_\theta(0) + \Delta A_\theta(\psi) = A_\theta(0) + c\psi^n \qquad (26)$$

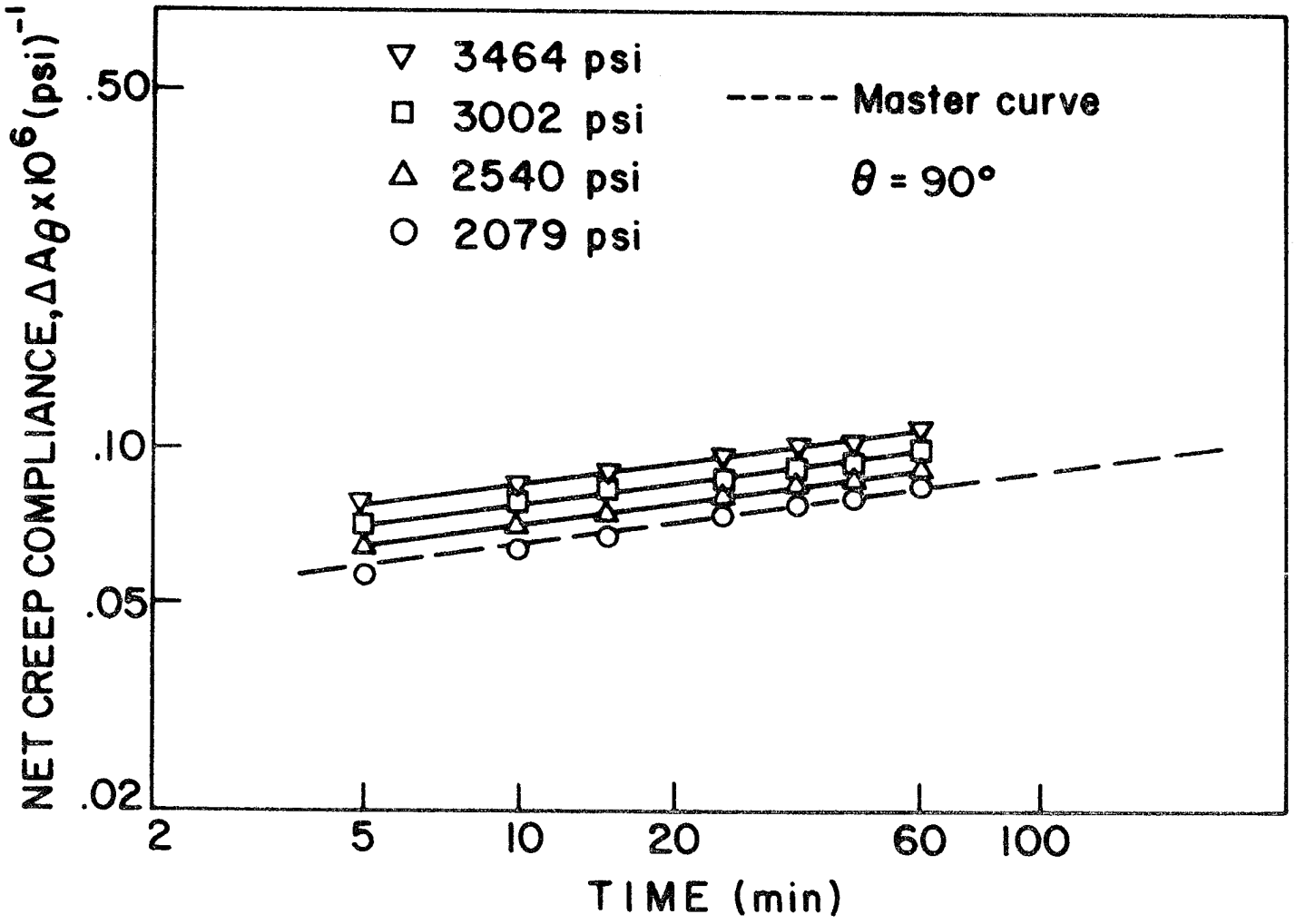

Figure 9. Net Creep Compliance for Different Stress Levels ($\theta = 90°$)

where $\psi = t/a_\sigma$ is stress-reduced time and c and n are independent of stress and time.

Substituting this power law (26) into equation (9b) yields

$$\varepsilon_r = g_2[c\psi^n - c(\psi-\psi_1)^n]\sigma_o \ , \ t > t_1 \tag{27}$$

and we derive the equation for normalized recovery strain

$$\frac{\varepsilon_r}{\Delta\varepsilon_1} = \frac{1}{g_1}[(1 + a_\sigma\lambda)^n - (a_\sigma\lambda)^n] \tag{28}$$

where

$$\lambda = \frac{t-t_1}{t_1}$$

Also

$$\Delta\varepsilon_1 = \varepsilon(t_1) - \varepsilon(0) = g_1 g_2 c\psi_1^n \sigma_o$$

is the transient component of strain existing immediately before the stress is removed.

Rewriting equation (28) we have,

$$\log(\frac{\varepsilon_r}{\Delta\varepsilon_1}) = -\log g_1 + \log[(1 + a_\sigma\lambda)^n - (a_\sigma\lambda)^n] \tag{29}$$

It is clear from equation (29) that a graphical shifting procedure can be applied to recovery data to determine a_σ and g_1 for different stress levels. For $\theta = 30^o$, it is estimated that n = .145 from Figure 8. A reference curve of normalized recovery strain $\frac{\varepsilon_r}{\Delta\varepsilon_1}$ is plotted against λ on double-logarithmic paper by letting $a_\sigma = g_1 = 1$ in equation (29). This reference curve is the normalized recovery strain for a linear viscoelastic material; it is shown as the solid line in Figure 10. Four normalized recovery curves of different stress levels are also shown in broken lines. It appears that they can be superposed on the reference (linear viscoelastic)

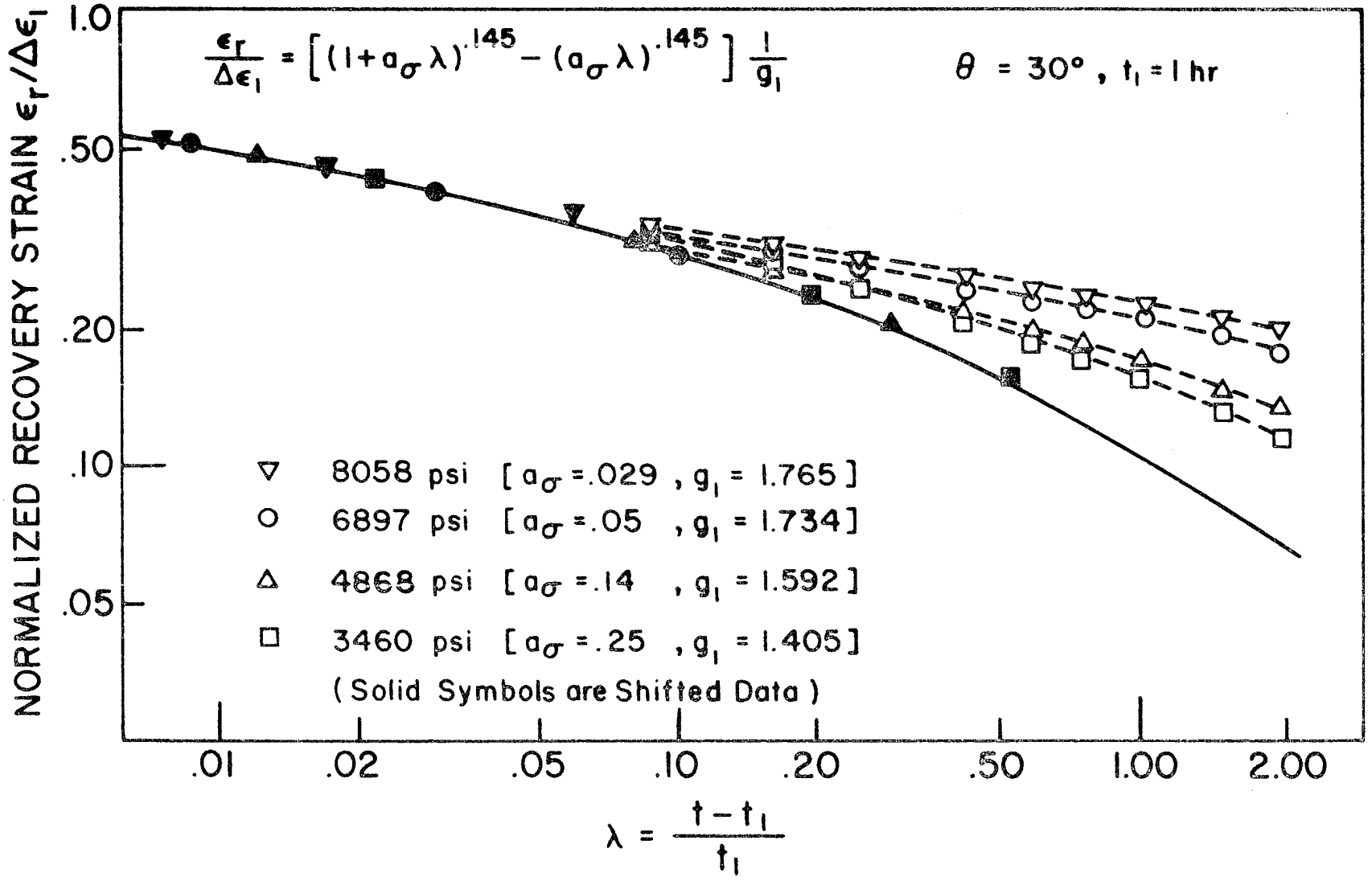

Figure 1. Determination for Shift Factors a_σ and g_1

curve by translating them along two axes, the amount of horizontal (λ) shift (to the left) and vertical ($\frac{\varepsilon_r}{\Delta\varepsilon_1}$) shift (up) is equal to - log a_σ and log g_1, respectively.

Since the curves shown in Figure 10 are not straight lines, unique values of a_σ and g_1 can be obtained by the shifting technique. After shifting, some of the data points for four different normalized recovery curves are shown as solid points on the reference curve. The ability to shift the data to the reference curve provides a check on the theory.

The normalized recovery curve for the lowest stress level (2069 psi) is not shown in Figure 10 since it was found to lie approximately on the curve of 3460 psi, and not on the reference curve. However, this does not mean the material is nonlinear at 2069 psi. Recall that the actual slope of the transient component of creep compliance at 2069 psi is not the same as the master curve in Figure 8; by using the actual slope of this creep compliance (n = 0.187) for predicting the reference recovery curve, we found that the measured recovery curve at 2069 psi lies approximately on this new reference curve; this result shows, therefore, that the material is essentially linear at the lowest stress of 2069 psi.

Given the values of log a_σ from the recovery Figure 10, the creep curves in Figure 8 are shifted this distance to the <u>right</u>. The additional amount of vertical shift needed to place each creep curve on the master curve (dashed line) gives the value of log $g_1 g_2$. Knowing g_1 from Figure 10, we then determine the value of g_2 at each stress.

This shifting procedure has been carried out for each stress level and fiber angle tested. The nonlinear properties are plotted in Figures 11, 12 and 13 against the "effective stress," σ_e, equation (16), which is

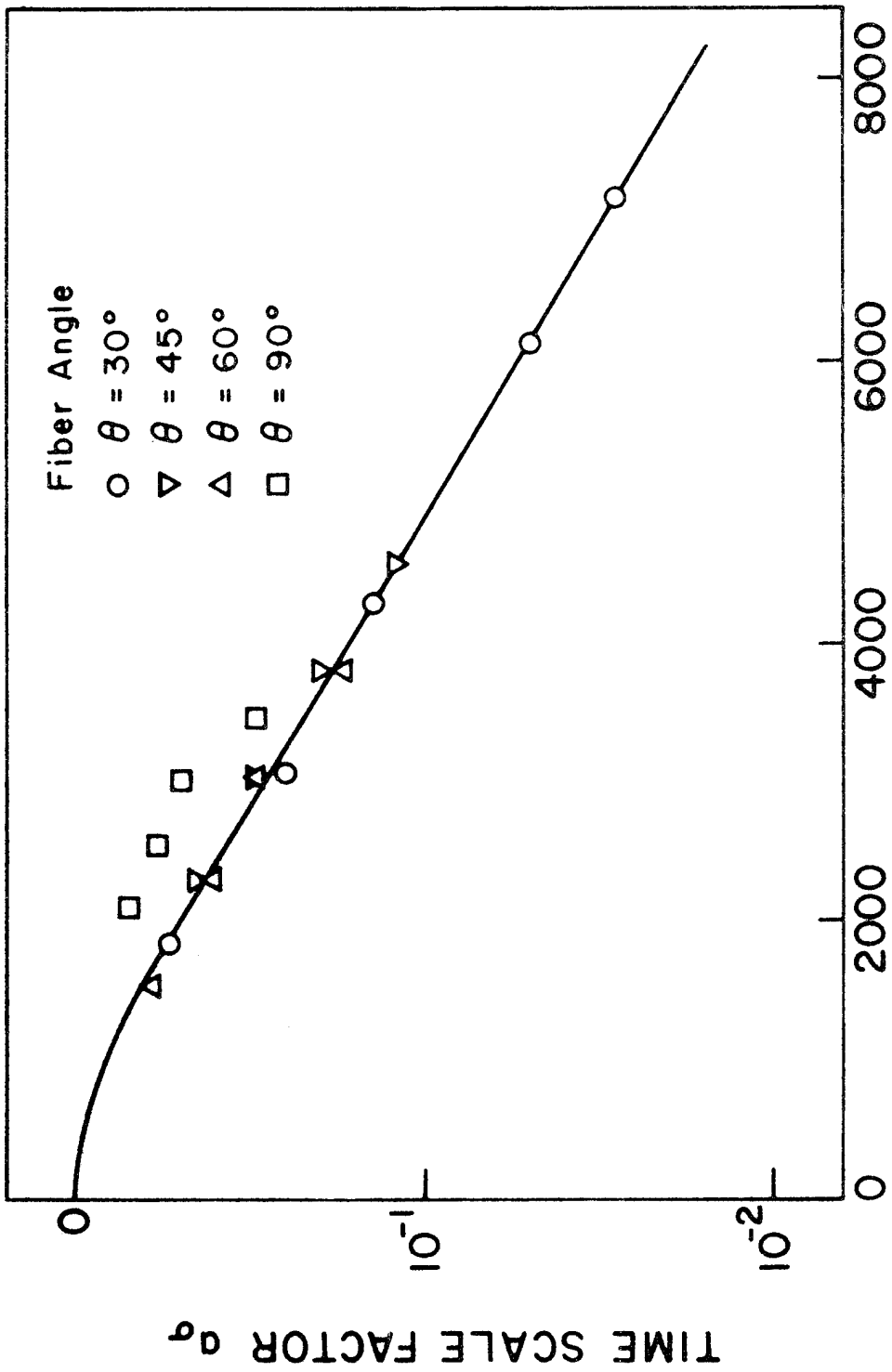

Figure 11. Shift factor a_σ

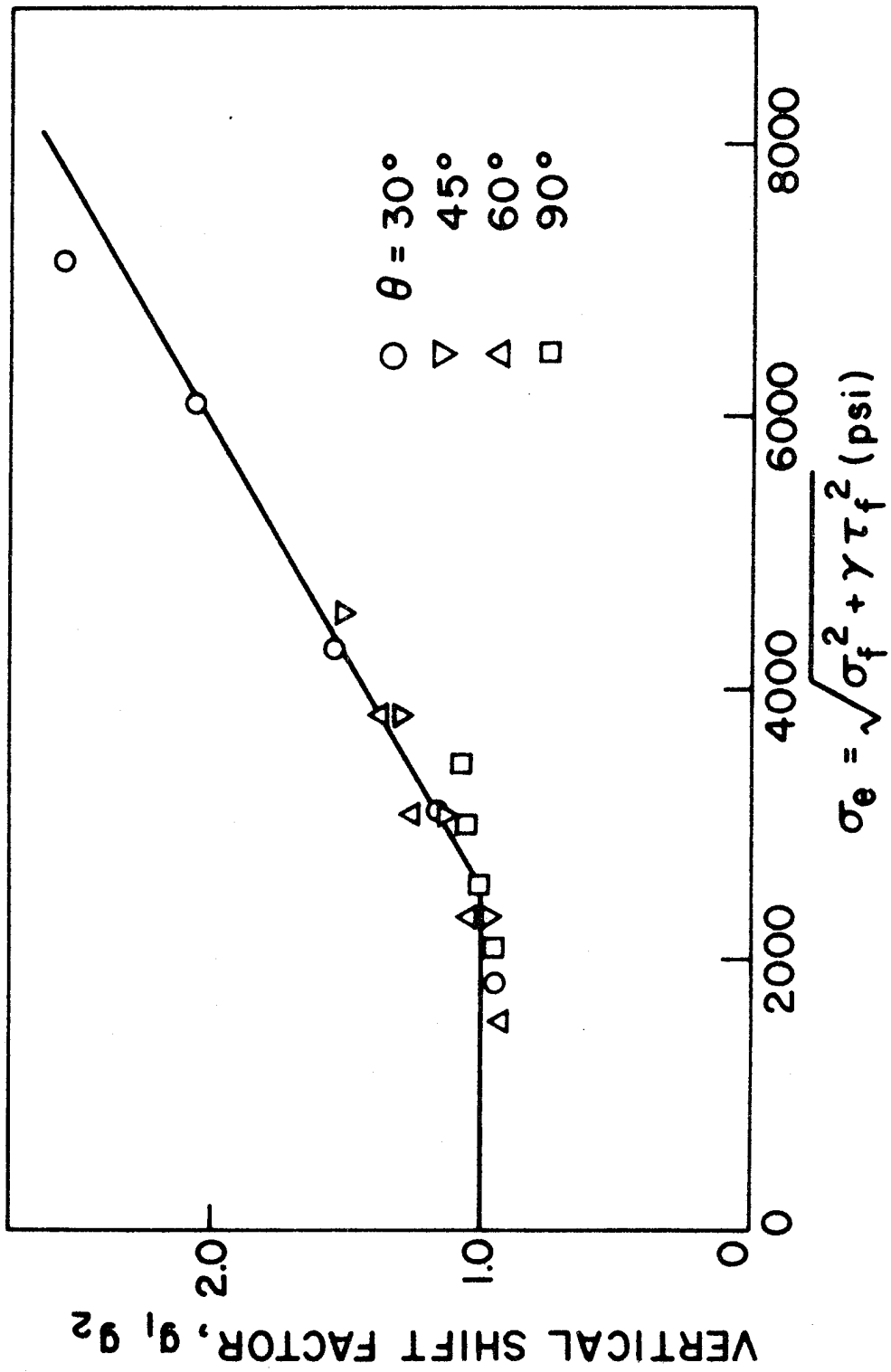

Figure 12. Shift Factor $g_1 g_2$

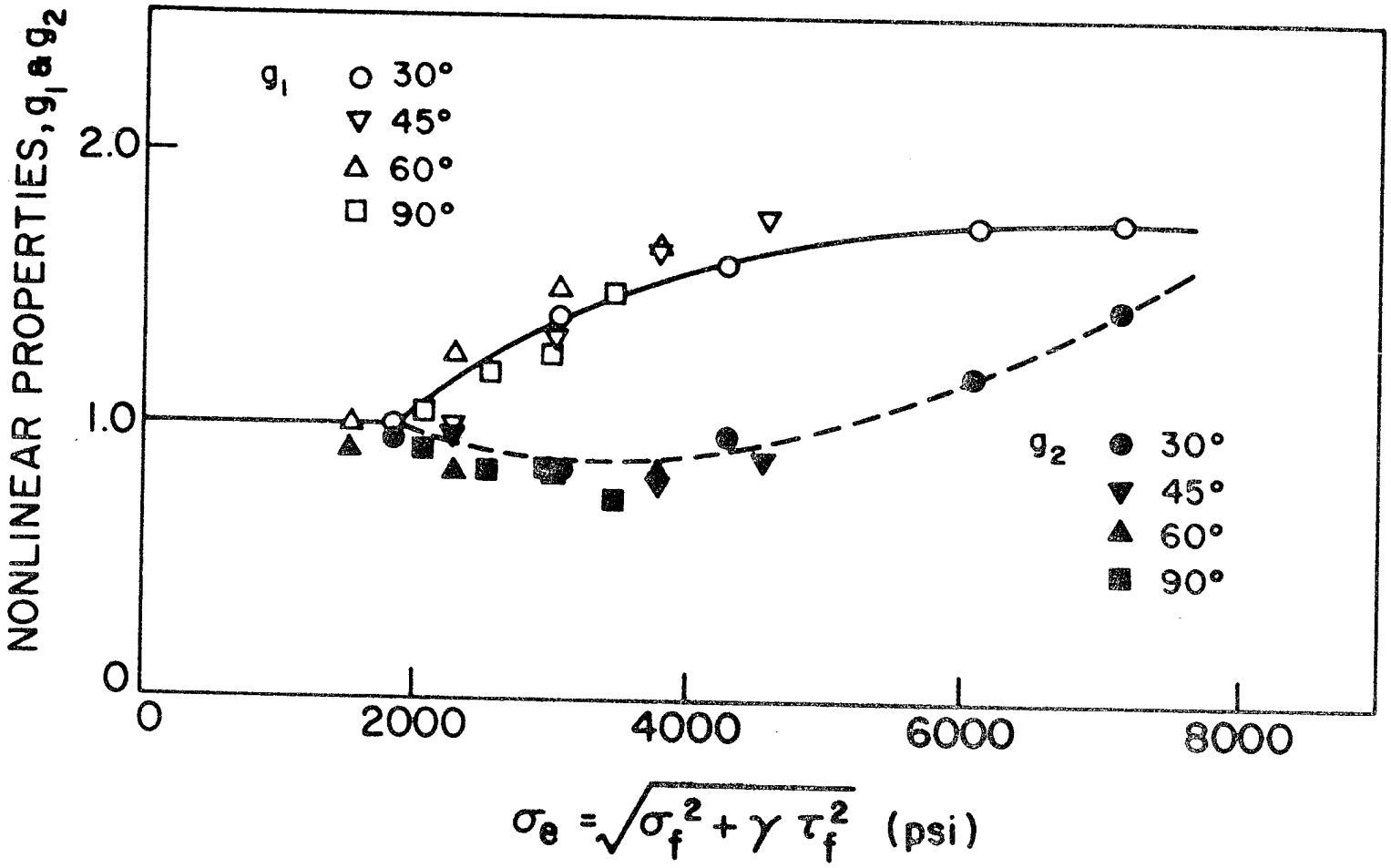

Figure 13. Nonlinear Material Properties g_1 and g_2

proportional to the average octahedral shear stress in the matrix. The constant value $\nu_e = 0.35$ was used to evaluate $\gamma = 3.88$, as discussed in Section II-3. The fact that most of the data fall on a single curve in each Figure indicates that σ_e is the principal factor causing nonlinearity.

Since $g_1 > 1$ in Figure 13, the jump of strain when $t = t_1$ is larger than that when $t = 0$; i.e. $\Delta\varepsilon_1 > g_o A(0)\sigma_o$ in equation (10).

The linear dependence of log a_σ on σ_e seen in Figure 11 at high stresses is especially interesting. This is the same behavior observed earlier for a glass-reinforced phenolic [4]; the fibers were in an orthogonal array, so that shear stress along the fibers, rather than σ_e, was found to be the principal invariant. This linearity in Figure 11 for the larger values of σ_e implies that

$$a_\sigma = Ae^{-B\sigma_e}$$

where A and B are positive constants. Exponential dependence is suggested by Eyring's rate process theory for high stresses when all nonlinearity is due to a_σ [9], but this molecular model is too simple to account for g_1 and g_2.

The transient components of recovery data are plotted against linear time scales in Figures 14 and 15 for the largest stresses applied at $\theta = 30^\circ$ and 90°. The accuracy of the recovery prediction is an indication of how close the shifted recovery data in Figure 10 are to the solid line. The modified superposition theory prediction, equation (8), was also made; note that equation (5a) can be used instead to make this prediction since it is valid for nonlinear behavior ($g_2 \neq 1$) when $g_o = g_1 = a_\sigma = 1$. Total strain using (5a) is shown in Figure 7. These results indicate that the modified superposition theory of Leaderman predicts recovery which is too rapid.

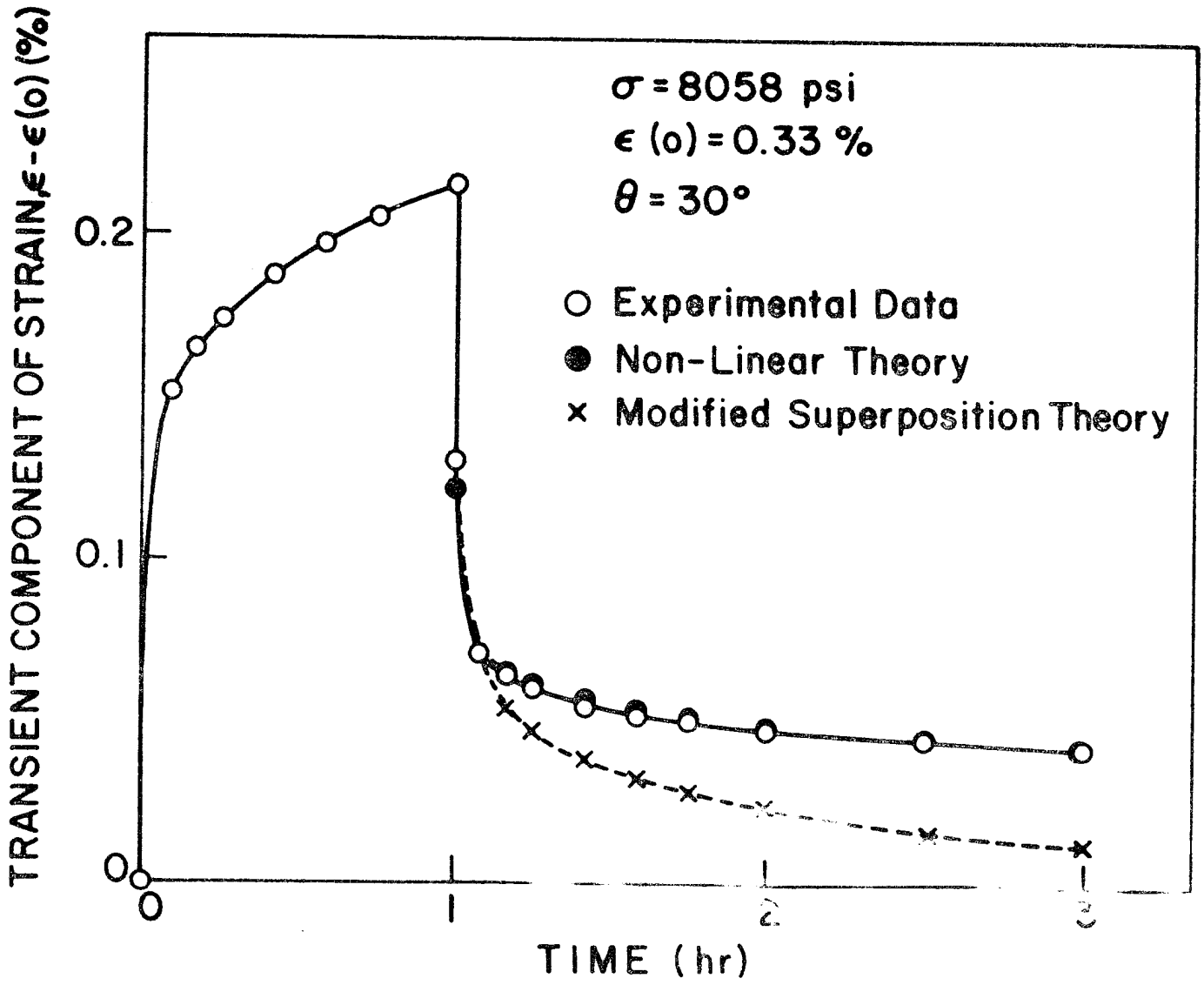

Figure 14. Net Creep-Recovery Curve ($\theta = 30^{\circ}$)

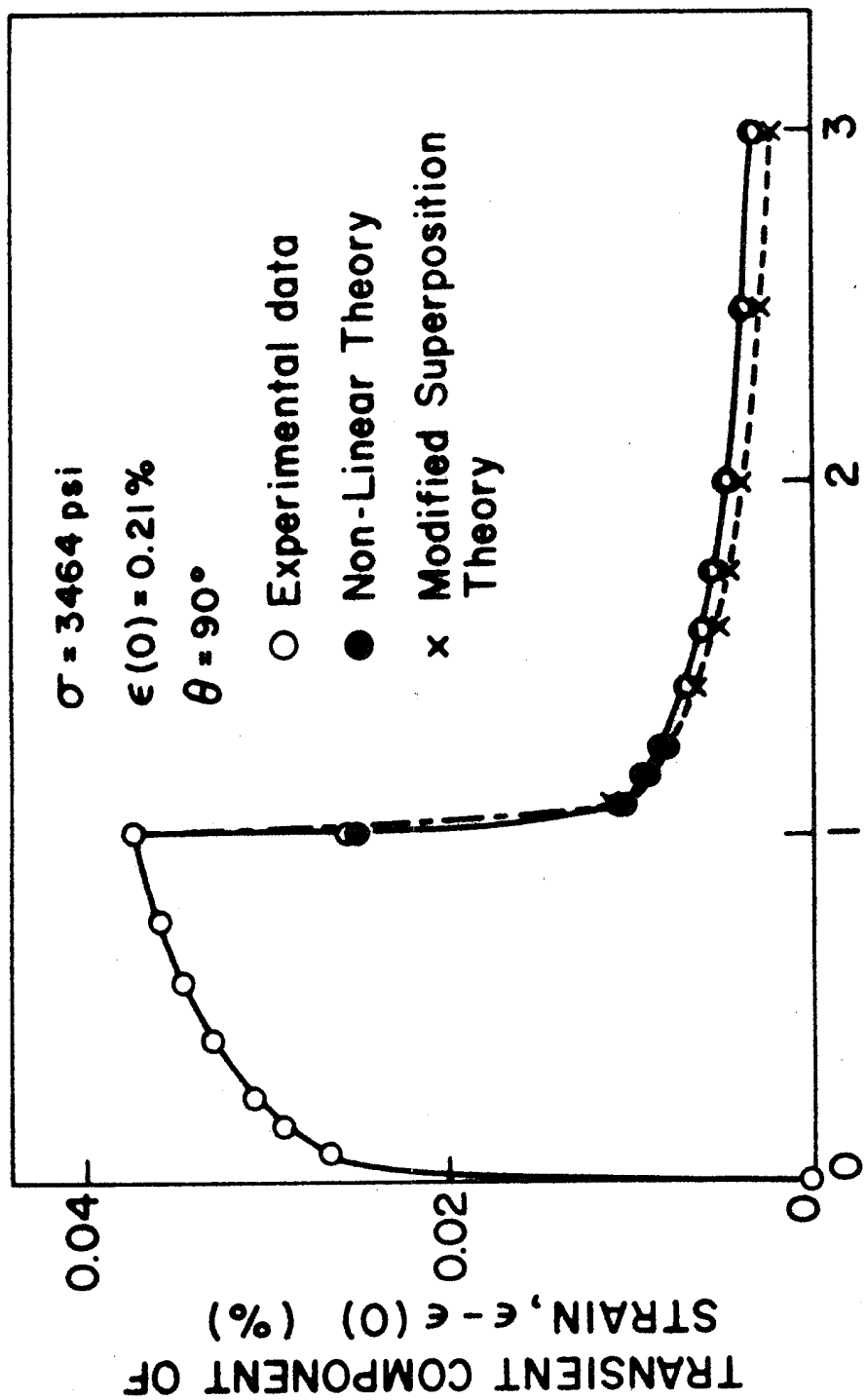

Figure 15. Net Creep-Recovery Curve ($\zeta = 90^{\circ}$)

d. Prediction of Creep Compliances

For the specimens $\theta = 90^\circ$, 45°, and 60°, we found that the material is approximately linearly viscoelastic up to stresses of 2079 psi, 2069 psi and 1345 psi, respectively. For the linear range, fourth order tensor transformation relations will be used to predict compliances at $\theta = 45^\circ$ and 60° given data at $\theta = 0^\circ$, 90°, and 30°. In order to predict compliances at higher stresses, one would simply bring in the values of g_1, g_2 and a_σ along with (9a); if all data points in Figures 11 and 12 were on a single curve, rather than being somewhat scattered, the predictions in the non-linear range would be as accurate as in the linear range.

First, we record the linear creep compliances found experimentally. They are

$$\begin{aligned}
A_o &= .184 \times 10^{-6} && (\text{psi}^{-1}) \\
A_{90} &= [.614 + .084\psi^{.145}] \times 10^{-6} && (\text{psi}^{-1}) \\
A_{30} &= [.410 + .062\psi^{.145}] \times 10^{-6} && (\text{psi}^{-1}) \\
A_{45} &= [.600 + .097\psi^{.132}] \times 10^{-6} && (\text{psi}^{-1}) \\
A_{60} &= [.668 + .107\psi^{.172}] \times 10^{-6} && (\text{psi}^{-1})
\end{aligned} \tag{30}$$

where ψ is stress-reduced time in hours; recall for the linear range $a_\sigma = 1$, so that $\psi = t$.

The transient components of the creep compliances ($\Delta A_\theta = A_\theta(\psi) - A_\theta(0) = c\psi^n$) have been plotted against ψ on double-logarithmic paper in Figure 16.

Since A_{ij} are fourth order tensor components, the standard transformation relations [7] give

$$A_\theta = (m^4 - 3m^2n^2)A_o + (n^4 - 1/3\ m^2n^2)A_{90} + \frac{16}{3} m^2n^2A_{30} \tag{31}$$

where

$$m = \cos\theta, \qquad n = -\sin\theta$$

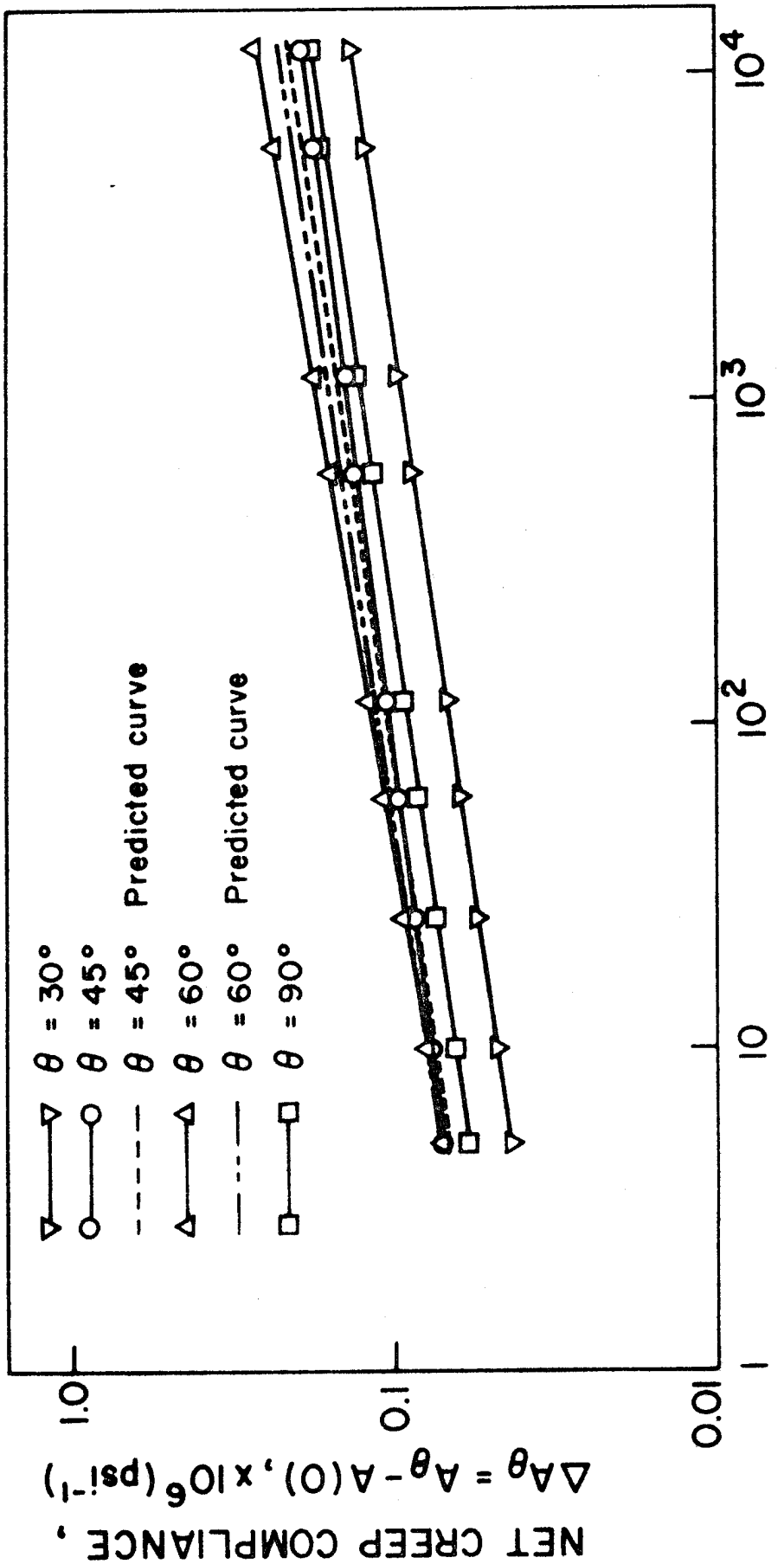

Figure 16. Transient Component of Linear Viscoelastic Creep Compliances

When $\theta = 45^{\circ}$ and 60°, we have

$$A_{45} = \frac{4}{3} A_{30} - \frac{1}{2} A_o + \frac{1}{6} A_{90} \tag{32a}$$

$$A_{60} = A_{30} - \frac{1}{2} A_o + \frac{1}{2} A_{90} \tag{32b}$$

By using the data obtained for A_o, A_{90}, A_{30} and equation (32), we predict A_{45} and A_{60}. They also have the power-law forms,

$$\begin{aligned} A'_{45} &= [.557 + .098\psi^{.145}] \times 10^{-6} \quad (\text{psi}^{-1}) \\ A'_{60} &= [.625 + .105\psi^{.145}] \times 10^{-6} \quad (\text{psi}^{-1}) \end{aligned} \tag{33}$$

The transient parts of the predicted A'_{45} and A'_{66} are shown in broken lines in Figure 16 to compare with the experimental results - compare also equations (33) with (30). For further comparison, 1 hour data of Figure 16 are plotted against fiber angle, θ, in Figure 6.

Part of the observed error is probably due to experimental errors and the lack of material homogeneity of the sheet from which the specimens were cut; also, small errors in the original estimates of initial compliances produce relatively large errors in the transient components, and could be one cause of the differences in slopes in Figure 16.

Section IV

PRINCIPAL CREEP COMPLIANCES

It was mentioned previously in Section III-2 that the principal creep compliances A_{11} and A_{22} are directly determined from axial strain measurements under uniaxial step stress input along the fibers and normal to the fibers, respectively; and the third principal creep compliance, A_{12}, can be measured by a strain gage placed transverse to the loading direction on a 0° or 90° specimen. They are found to be independent of stress and have the values,

$$\begin{aligned} A_{11} &= A_{o} = .184 \times 10^{-6} && (psi^{-1}) \\ A_{22} &= A_{90} = [.614 \times .084\psi^{.145}] \times 10^{-6} && (psi^{-1}) \\ A_{12} &= A_{21} = -.057 \times 10^{-6} && (psi^{-1}) \end{aligned} \tag{34}$$

The fourth principal creep compliance A_{66} can be calculated by using the data of A_{11}, A_{22}, A_{12} and A_{30}, and the standard tensor transformation relation [7]:

$$A_{66} = \frac{16}{3} A_{30} - 3A_{11} - 2A_{12} - \frac{1}{3} A_{22} \tag{35}$$

The resulting four principal creep compliances are plotted against log ψ in Figure 17. These four compliances completely characterize linear viscoelastic behavior under all states of plane stress.

Earlier we said equation (20) is only an approximation because of specimen bending that exists with off-angle specimens. Now we want to check this approximation. By using the principal data and tensor transformation

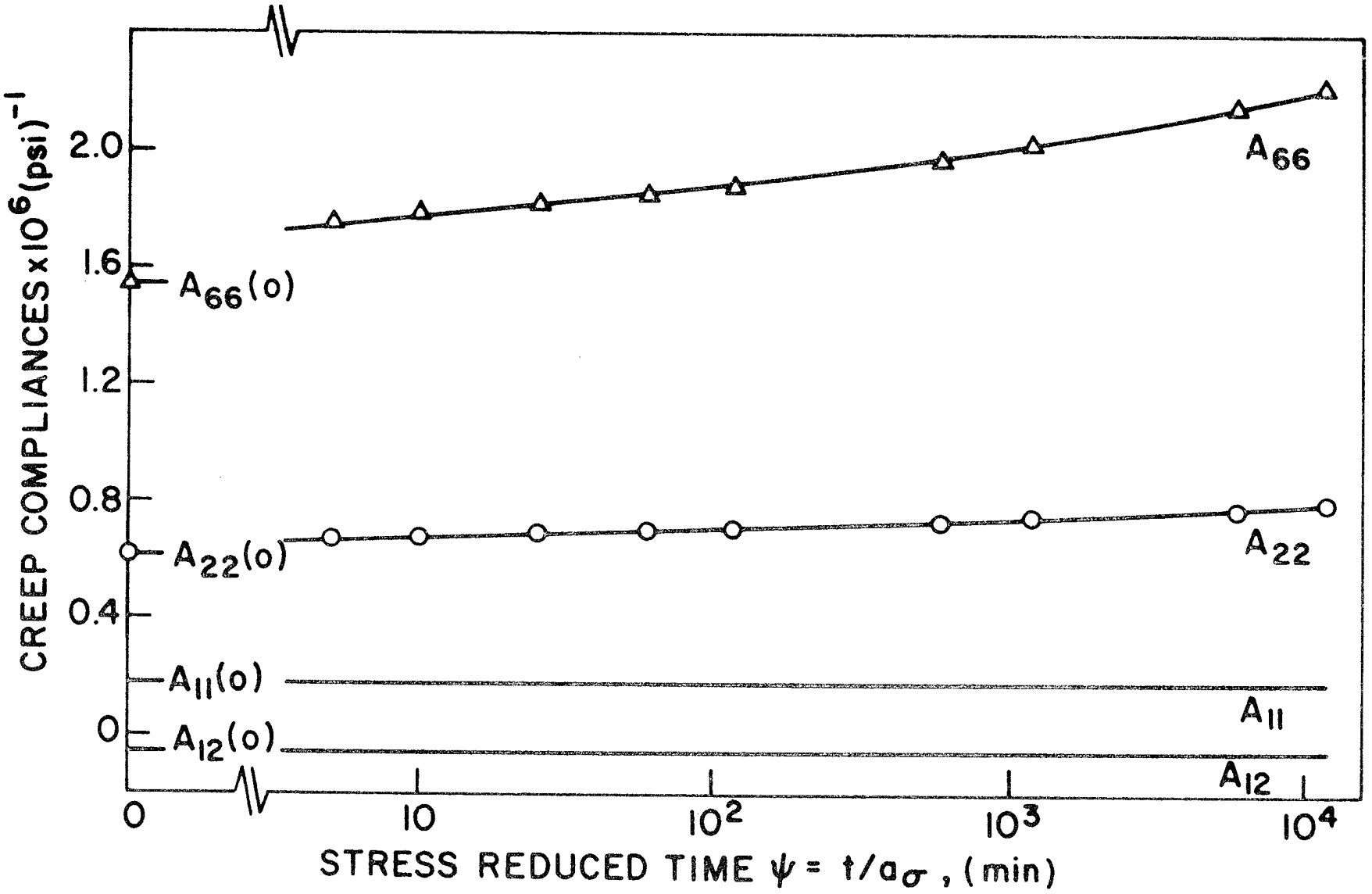

Figure 17. Principal Creep Compliances

relations we can calculate the compliance A_{30}, which would be measured if the material really had the principal creep compliances above. It appears that the approximation is very good, with the directly measured value A_{30} as shown in Table 1.

Table I

Comparison of the measured and calculated A_{30}.

ψ (Hrs)	Measured $A_{30} \times 10^6$ $(psi)^{-1}$	Calculated $A_{30} \times 10^6$ $(psi)^{-1}$
0	.410	.407
1	.472	.468
20	.507	.502
200	.547	.541

Section V

MULTIPLE-STEP LOADING

The nonlinear theory has been successfully applied to creep and recovery data reduction and prediction in the previous Sections. This theory will now be used to predict response under multiple-step loading and then compared to test data for the $\theta = 30^{\circ}$ specimen.

The constitutive equation (6) is used to make this prediction,

$$\varepsilon = g_o A(0)\sigma + g_1 \int_o^t \Delta A(\psi-\psi') \frac{dg_2\sigma}{d\tau} d\tau \qquad (6)$$

where

$$\psi = \int_o^t d\tau/a_\sigma$$

The two-step loading and two-step unloading program shown in Figure 18 was chosen.

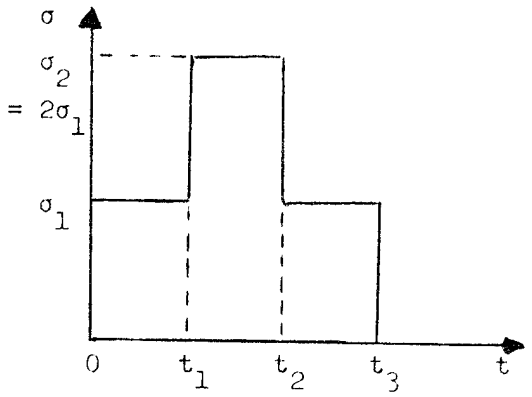

Figure 18

Multiple-Step Loading Program

The stress input function $g_2\sigma$ has the form,

$$g_2\sigma = g_2^1\sigma_1 H(\tau) + (g_2^2\sigma_2 - g_2^1\sigma_1)H(\tau-t_1)$$

$$-(g_2^2\sigma_2 - g_2^1\sigma_1)H(\tau-t_2) - g_2^1\sigma_1 H(\tau-t_3) \qquad (36)$$

The related nonlinear properties a_σ, g_1 and g_2 have a similar form; for example,

$$a_\sigma = 1 + (a_\sigma^1 - 1)H(\tau) + (a_\sigma^2 - a_\sigma^1)H(\tau-t_1)$$

$$-(a_\sigma^2 - a_\sigma^1)H(\tau-t_2) - (a_\sigma^1 - 1)H(\tau-t_3) \qquad (37)$$

where the superscript on a material property indicates the particular stress at which it is to be evaluated.

Substituting the stress history (36) into equation (6), and using the related nonlinear properties, e.g. (37), yields,

for $0 < t < t_1$

$$\varepsilon = g_o^1 A(0)\sigma_1 + g_1^1 g_2^1 \Delta A(\psi)\sigma_1 \qquad (38a)$$

$$\psi = t/a_\sigma^1$$

for $t_1 < t < t_2$

$$\varepsilon = g_o^2 A(0)\sigma_2 + g_1^2[g_2^1\sigma_1\Delta A(\psi) + (g_2^2\sigma_2 - g_2^1\sigma_1)\Delta A(\psi-\psi_1)]$$

$$\psi = t_1/a_\sigma^1 + (t-t_1)/a_\sigma^2$$

$$\psi-\psi_1 = (t-t_1)/a_\sigma^2 \qquad (38b)$$

for $t_2 < t < t_3$

$$\varepsilon = g_o^1 A(0)\sigma_1 + g_1^1[g_2^1\sigma_1\Delta A(\psi) + (g_2^2\sigma_2 - g_2^1\sigma_1)\Delta A(\psi-\psi_1)$$

$$-(g_2^2\sigma_2 - g_2^1\sigma_1)\Delta A(\psi-\psi_2)] \qquad (38c)$$

$$\psi = t_1/a_\sigma^1 + (t_2-t_1)/a_\sigma^2 + (t-t_2)/a_\sigma^1$$

$$\psi-\psi_1 = (t_2-t_1)/a_\sigma^2 + (t-t_2)/a_\sigma^1$$

$$\psi-\psi_2 = (t-t_2)/a_\sigma^1$$

for $t_3 < t$,

$$\varepsilon = g_2^1\sigma_1\Delta A(\psi) + (g_2^2\sigma_2 - g_2^1\sigma_1)\Delta A(\psi-\psi_1)$$

$$-(g_2^2\sigma_2 - g_2^1\sigma_1)\Delta A(\psi-\psi_2) - g_2^1\sigma_1\Delta A(\psi-\psi_3) \qquad (38d)$$

$$\psi = t_1/a_\sigma^1 + (t_2-t_1)/a_\sigma^2 + (t_3-t_2)/a_\sigma^1 + (t-t_3)$$

$$\psi-\psi_1 = (t_2-t_1)/a_\sigma^2 + (t_3-t_2)/a_\sigma^1 + (t-t_3)$$

$$\psi-\psi_2 = (t_3-t_2)/a_\sigma^1 + (t-t_3)$$

$$\psi-\psi_3 = t-t_3$$

The actual stress and time values used are σ_1 = 3460 psi, σ_2 = 6920 psi, and t_1 = 1/2 hr, t_2 = 1 hr, t_3 = 1.5 hr. The test was made twice on the same 30° specimen at 164°F and 21% relative humidity used to characterize the material. The linear creep compliance and the stress-dependent nonlinear properties, which we obtained previously from data reduction procedures, are used in equations (38) to predict the strain response. The results for the second repetition of this load history,only slightly different from those of the first load history, are shown in Figure 19 and seen to agree very well with the experimental observations except for the third region ($t_2 < t < t_3$). This figure shows that the agreement is much better than achieved using linear theory.

The data in Figure 19 were obtained several weeks after the specimen was characterized. Therefore, some of the error can probably be attributed to the long rest period and resulting change in properties.

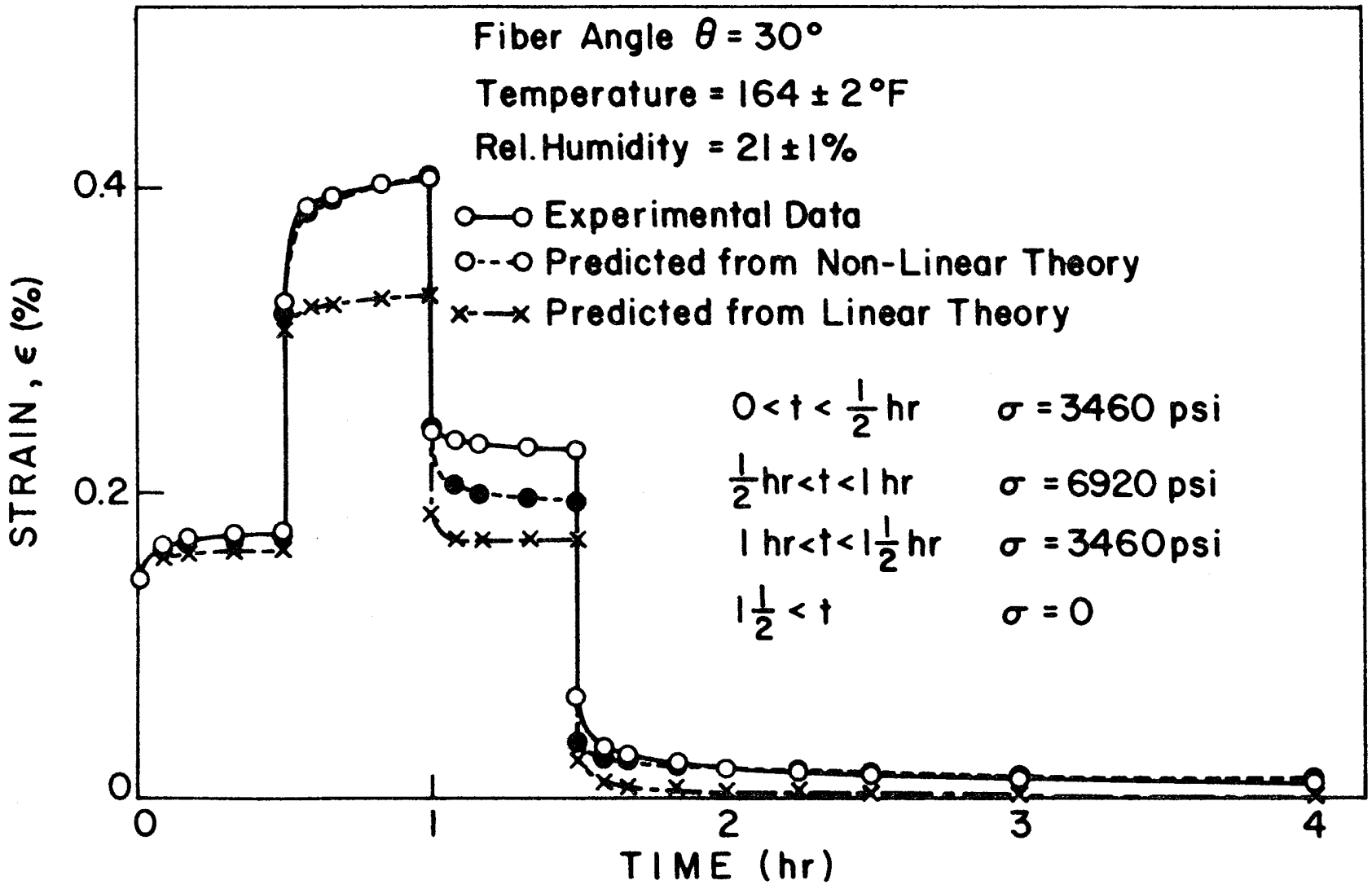

Figure 19. Strain Response to Multiple-Step Loading

Section VI

CONCLUSIONS

An appreciable amount of nonlinearity in the transient component of strain was found to exist in all specimens, except for those under loading parallel to the fibers. The nonlinear constitutive equation (6) derived from thermodynamic theory [1] has been used successfully to characterize the glass fiber-epoxy composite under uniaxial loading; although only a uniaxial equation has been given here, multiaxial relations have been derived [1]. Linear viscoelastic compliances and nonlinear properties were evaluated by applying graphical shifting procedures to creep and recovery data. All three nonlinear properties, g_1, g_2, and a_σ were found to be a function of essentially only one mechanical invariant: the average octahedral shear stress in the epoxy matrix.

Such a result seems to indicate uniaxial creep and recovery tests may be sufficient to characterize the composite for multiaxial stress applications. However, the conclusion is very preliminary at this time, as other functions in [1] may enter and confirmation from a multiaxial-stress test program is needed.

The nonlinear theory used in this report is applied more easily than the familiar multiple-integral representation in characterizing a nonlinear viscoelastic solid. The single-integral form makes it relatively easy to use in engineering stress analysis applications as well. Moreover, the only time-dependent functions which appear in the constitutive theory are the linear viscoelastic creep compliances.

Some error was observed in predicting the angular dependence of the compliances and strain response to multiple-step loading. It is believed that possible sources of the error, in addition to specimen-to-specimen property variations and experimental error, are the method used to estimate initial compliance and a gradual change in properties observed for a single specimen under repeated loading and unloading.

Motivated by this finding, a new data reduction procedure has been developed without restricting $g_o = 1$ [12]; recovery data is utilized in estimating the initial compliance. This new method provides better agreement with respect to angular dependence of the compliance but does not appreciably change the response under multiple-step loading.

The effect of temperature on material properties is not covered in the present report, but [12] does include some results at various temperatures.

ACKNOWLEDGEMENT

The authors are indebted to Professor E. O. Stitz for providing valuable assistance in the experimental phase of the research program.

REFERENCES

1. R. A. Schapery, "Further Development of a Thermodynamic Constitutive Theory: Stress Formulation," Purdue University, Rept. No. 69-2 (February 1969).
2. H. Leaderman, "Elastic and Creep Properties of Filamentous Materials and Other High Polymers," The Textile Foundation, Washington,D. C. (1943).
3. W. N. Findley and J. S. Y. Lai, "A Modified Superposition Principle Applied to Creep of Nonlinear Viscoelastic Materials Under Abrupt Changes in State of Combined Stress," Trans. Soc. Rheol., 11, 361 (1967).
4. R. A. Schapery, "On the Characterization of Nonlinear Viscoelastic Materials," J. Polymer Engineering and Sciences (July 1969).
5. Y. C. Fung, "Fundamentals of Solid Mechanics," Englewood Cliffs, New Jersey, Prentice-Hall (1965).
6. J. C. Halpin, "Introduction to Viscoelasticity," in Composite Materials Workshop, S. W. Tsai, J. C. Halpin, and N. J. Pagano, Eds., Technomic (1968).
7. J. E. Ashton, J. C. Halpin,and P. H. Petit, "Primer on Composite Materials: Analysis," Stamford,Conn., Technomic (1969).
8. N. J. Pagano and J. C. Halpin, "Influence of End Constraint in the Testing of Anisotropic Bodies," J. Comp. Mat., Vol. 2 (1968), p.18.
9. R. L. Thorkildsen, "Mechanical Behavior," Ch. 5 in Engineering Design for Plastics, Eric Baer, Ed., Reinhold (1964).

10. M. M. Martirosyan, "Transient Creep of Glass-Reinforced Plastic," Mekhanika Polimerov, 1 47 (1965).

11. R. A. Schapery, "Stress Analysis of Viscoelastic Composite Materials," J. Composite Materials, 1 228 (1967).

12. Y. C. Lou and R. A. Schapery, "Viscoelastic Characterization of a Nonlinear, Fiber-Reinforced Plastic," to be published in J. Composite Materials (1969).

APPENDIX I

On the Application of a Thermodynamic Constitutive Equation to Various Nonlinear Materials*

R. A. Schapery

ABSTRACT

The author's thermodynamic constitutive theory for nonlinear viscoelastic behavior is extended to account for rate-independent plastic flow and for nonlinear creep with strong stress-dependence. The resulting constitutive equation is then applied to several different materials under small and large strains in order to bring out the significance of the nonlinear functions, and to obtain a check on the theory. History effects are accounted for by means of a single integral which is very similar to the Boltzmann form in linear theory, and therefore permits easy application to the various loading and straining conditions studied. On the basis of physical arguments and some example applications to glassy and polycrystalline materials, including fiber-reinforced plastic, it is suggested that nonlinear, multiaxial response of these solids can often be described by linear viscoelastic equations with an intrinsic time-scale that is affected by mechanical invariants and temperature; for example, the classical three-dimensional stress-strain equations of rate-independent, incremental plasticity and nonlinear creep of metals are shown to be included in this description. Only a slightly more involved form is needed to characterize a number of unfilled and filled soft polymers under finite strain.

---

* Presented at the IUTAM Symposium on Thermoinelasticity, East Kilbride, Scotland, June 26-28, 1968. (To be published in Proceedings.) Work was originally published as Purdue University Report No. AA&ES 68-4 (June 1968).

APPENDIX II

Thermal Expansion Coefficients of Composite Materials Based on Energy Principles*

R. A. Schapery

ABSTRACT

Bounds on effective thermal expansion coefficients of isotropic and anisotropic composite materials consisting of isotropic phases are derived by employing extremum principles of thermoelasticity. Inequalities between certain approximate and exact forms of the potential and complementary energy functionals are first established. These inequalities are then used in conjunction with a new method for minimizing the difference between upper and lower bounds in order to derive volumetric and linear thermal expansion coefficients. Application is made to two- and three-phase isotropic composites and a fiber-reinforced material. It is found for some important cases that the solutions are exact, and take a very simple form. We also show conditions under which the rule-of-mixtures and Turner's equation can be used for thermal expansion coefficients. Finally, simple methods for extending all results to viscoelastic composites are indicated.

*Published in J. Composite Materials, Vol. 2, pp. 380-404 (July 1968).

UNCLASSIFIED

Security Classification

DOCUMENT CONTROL DATA - R&D

(Security classification of title, body of abstract and indexing annotation must be entered when the overall report is classified)

1. ORIGINATING ACTIVITY *(Corporate author)*

Purdue University
Lafayette, Indiana

2a. REPORT SECURITY CLASSIFICATION

UNCLASSIFIED

2b. GROUP

3. REPORT TITLE

Viscoelastic Behavior of a Nonlinear Fiber-Reinforced Plastic

4. DESCRIPTIVE NOTES *(Type of report and inclusive dates)*

Final - 1 January 1968 to 31 December 1968

5. AUTHOR(S) *(Last name, first name, initial)*

Lou, Y. C.; Schapery, R. A.

6. REPORT DATE	7a. TOTAL NO. OF PAGES	7b. NO. OF REFS
April 1969	54	12

8a. CONTRACT OR GRANT NO.	9a. ORIGINATOR'S REPORT NUMBER(S)
F33615-67-C-1412	AFML-TR-68-90, Part II
b. PROJECT NO. 7342 Task No. 7342002	9b. OTHER REPORT NO(S) *(Any other numbers that may be assigned this report)*
c.	
d.	

10. AVAILABILITY/LIMITATION NOTICES

This document has been approved for public release and sale; its distribution is unlimited.

11. SUPPLEMENTARY NOTES	12. SPONSORING MILITARY ACTIVITY
	Air Force Materials Laboratory Air Force Systems Command Wright-Patterson AFB, Ohio 45433

13. ABSTRACT

The nonlinear mechanical properties of a unidirectional, glass fiber-epoxy composite at 164°F are characterized by using creep and recovery tests together with a constitutive equation based on a thermodynamic theory. Our experimental effort covers studies on specimens with fiber orientations at $\theta = 0^\circ$, 30°, 60°, and 90° with respect to the uniaxial loading direction. The results for $\theta = 0$ specimen show that the composite is linearly elastic for the load range studied, but nonlinear viscoelastic behavior is observed for the other orientations. Guided by the nonlinear constitutive equation, the creep and recovery data are plotted on double-logarithmic paper, and the material properties are found by shifting the data to form a "master curve" for each fiber orientation. Prediction of master curves of $\theta = 45^\circ$ and 60° from master curves of $\theta = 0^\circ$, 90°, and 30° is made. Four principal creep compliances are estimated by using the master curves and tensor transformation relations. Finally, we use the nonlinear equation to predict strain response due to multiple-step loading and unloading.

The Appendix contains two abstracts of papers which were completed and published during the period covered by this report.

DD FORM 1 JAN 64 1473

UNCLASSIFIED

Security Classification

14. KEY WORDS	LINK A		LINK B		LINK C	
	ROLE	WT	ROLE	WT	ROLE	WT
Nonlinear Mechanical Properties Constitutive Equations Viscoelastic Behavior Glass Fiber - Epoxy Composite Uniaxial Loading						

INSTRUCTIONS

1. ORIGINATING ACTIVITY: Enter the name and address of the contractor, subcontractor, grantee, Department of Defense activity or other organization *(corporate author)* issuing the report.

2*a*. REPORT SECURITY CLASSIFICATION: Enter the overall security classification of the report. Indicate whether "Restricted Data" is included. Marking is to be in accordance with appropriate security regulations.

2*b*. GROUP: Automatic downgrading is specified in DoD Directive 5200.10 and Armed Forces Industrial Manual. Enter the group number. Also, when applicable, show that optional markings have been used for Group 3 and Group 4 as authorized.

3. REPORT TITLE: Enter the complete report title in all capital letters. Titles in all cases should be unclassified. If a meaningful title cannot be selected without classification, show title classification in all capitals in parenthesis immediately following the title.

4. DESCRIPTIVE NOTES: If appropriate, enter the type of report, e.g., interim, progress, summary, annual, or final. Give the inclusive dates when a specific reporting period is covered.

5. AUTHOR(S): Enter the name(s) of author(s) as shown on or in the report. Enter last name, first name, middle initial. If military, show rank and branch of service. The name of the principal author is an absolute minimum requirement.

6. REPORT DATE: Enter the date of the report as day, month, year; or month, year. If more than one date appears on the report, use date of publication.

7*a*. TOTAL NUMBER OF PAGES: The total page count should follow normal pagination procedures, i.e., enter the number of pages containing information.

7*b*. NUMBER OF REFERENCES: Enter the total number of references cited in the report.

8*a*. CONTRACT OR GRANT NUMBER: If appropriate, enter the applicable number of the contract or grant under which the report was written.

8*b*, 8*c*, & 8*d*. PROJECT NUMBER: Enter the appropriate military department identification, such as project number, subproject number, system numbers, task number, etc.

9*a*. ORIGINATOR'S REPORT NUMBER(S): Enter the official report number by which the document will be identified and controlled by the originating activity. This number must be unique to this report.

9*b*. OTHER REPORT NUMBER(S): If the report has been assigned any other report numbers *(either by the originator or by the sponsor)*, also enter this number(s).

10. AVAILABILITY/LIMITATION NOTICES: Enter any limitations on further dissemination of the report, other than those imposed by security classification, using standard statements such as:

(1) "Qualified requesters may obtain copies of this report from DDC."

(2) "Foreign announcement and dissemination of this report by DDC is not authorized."

(3) "U. S. Government agencies may obtain copies of this report directly from DDC. Other qualified DDC users shall request through

_____."

(4) "U. S. military agencies may obtain copies of this report directly from DDC. Other qualified users shall request through

_____."

(5) "All distribution of this report is controlled. Qualified DDC users shall request through

_____."

If the report has been furnished to the Office of Technical Services, Department of Commerce, for sale to the public, indicate this fact and enter the price, if known.

11. SUPPLEMENTARY NOTES: Use for additional explanatory notes.

12. SPONSORING MILITARY ACTIVITY: Enter the name of the departmental project office or laboratory sponsoring *(paying for)* the research and development. Include address.

13. ABSTRACT: Enter an abstract giving a brief and factual summary of the document indicative of the report, even though it may also appear elsewhere in the body of the technical report. If additional space is required, a continuation sheet shall be attached.

It is highly desirable that the abstract of classified reports be unclassified. Each paragraph of the abstract shall end with an indication of the military security classification of the information in the paragraph, represented as *(TS), (S), (C), or (U)*.

There is no limitation on the length of the abstract. However, the suggested length is from 150 to 225 words.

14. KEY WORDS: Key words are technically meaningful terms or short phrases that characterize a report and may be used as index entries for cataloging the report. Key words must be selected so that no security classification is required. Identifiers, such as equipment model designation, trade name, military project code name, geographic location, may be used as key words but will be followed by an indication of technical context. The assignment of links, rules, and weights is optional.